Mitochondrial stress in GABAergic neurons non-cell autonomously regulates organismal

2 health and aging

1

3

6

7

17

- 4 Laxmi Rathor¹, Shayla Curry¹, Youngyong Park^{2,3}, Taylor McElroy¹, Briana Robles¹, Yi Sheng¹,
- 5 Wei-Wen Chen⁴, Kisuk Min⁵, Rui Xiao¹, Myon Hee Lee^{3,6}, and Sung Min Han^{1†}

Affiliations

- 8 Department of Physiology and Aging, College of Medicine, University of Florida, Gainesville, FL
- 9 32610, USA
- ² Division of Hematology/Oncology, Department of Internal Medicine, Brody School of Medicine
- at East Carolina University, Greenville, NC 27834, USA
- ³ Department of Biology, Johns Hopkins University, Baltimore, MD, 21218, USA
- ⁴ School of Chemistry & Biochemistry, College of Sciences, Georgia Institute of Technology,
- 14 Atlanta, GA 30332, USA
- 15 Department of Kinesiology, University of Texas at El Paso, El Paso, TX 79968, USA
- 16 begin begin

18 [†]Corresponding author:

- 19 Sung Min Han, Ph.D.
- 20 Department of Physiology and Aging, Institute on Aging, College of Medicine, University of Florida,
- 21 Gainesville, Florida 32610, USA.
- 22 Tel.: 352-273-5682, Fax: 352-273-5737, Email: han.s@ufl.edu.

Abstract

Mitochondrial stress within the nervous system can trigger non-cell autonomous responses in peripheral tissues. However, the specific neurons involved and their impact on organismal aging and health have remained incompletely understood. Here, we demonstrate that mitochondrial stress in γ-aminobutyric acid-producing (GABAergic) neurons in *Caenorhabditis elegans* (*C. elegans*) is sufficient to significantly alter organismal lifespan, stress tolerance, and reproductive capabilities. This mitochondrial stress also leads to significant changes in mitochondrial mass, energy production, and levels of reactive oxygen species (ROS). DAF-16/FoxO activity is enhanced by GABAergic neuronal mitochondrial stress and mediates the induction of these non-cell-autonomous effects. Moreover, our findings indicate that GABA signaling operates within the same pathway as mitochondrial stress in GABAergic neurons, resulting in non-cell-autonomous alterations in organismal stress tolerance and longevity. In summary, these data suggest the crucial role of GABAergic neurons in detecting mitochondrial stress and orchestrating non-cell-autonomous changes throughout the organism.

Keywords

Mitochondria, GABAergic neurons, GABA, aging, healthspan, reproduction, DAF-16/FoxO

Introduction

Mitochondria are essential organelles involved in various cellular functions, including energy production, calcium regulation, cell signaling, and apoptosis. Their reciprocal relationship with aging is widely acknowledged, wherein mitochondrial dysfunction impacts organismal longevity and health, and aging affects mitochondrial homeostasis across variable model animals ^{1, 2}. The degree of mitochondrial dysfunction determines the effect on an organismal lifespan. Mild mitochondrial disruption has been shown to increase lifespan in model animals such as *C. elegans*, flies, and mice ³⁻¹⁰. For instance, the lifespan of *C. elegans* is extended by inhibiting mitochondria-related genes through genetic and RNA interference (RNAi) knockdown, including *isp-1* (an iron-sulfur subunit of complex III of the mitochondrial electron transport chain (ETC)) ⁶, *spg-7* (a mitochondrial quality control m-AAA protease) ¹¹⁻¹³, and *clk-1* (a hydroxylase involved in the biosynthesis of ubiquinone) ^{5, 14}. Like *C. elegans clk-1* mutant, mice with the *mclk1* mutation, which exhibits normal growth and fertility, also exhibits an increase in lifespan ¹⁵.

The mechanisms underlying longevity enhancements through mitochondrial perturbations bring forth the mitohormesis theory that enhanced stress response pathways contribute to longer lifespans ^{4, 16-21}. It has been demonstrated that some mitochondrial stress requires the mitochondrial unfolded protein response (mitoUPR) pathway to trigger lifespan extension ^{4, 16-19}. The forkhead transcription factor DAF-16/FoxO has also been reported as an additional mediator responsible for extending the lifespan of *C. elegans* ETC mutants ^{20, 21}. However, certain mitochondrial perturbations and mutations in ETC genes can independently extend lifespan without involving *atfs-1*, a key regulator of mitoUPR ^{17, 22}. Similarly, it has been documented that DAF-16/FoxO is not indispensable in mediating the lifespan extension in some ETC mutants ⁶, suggesting a complex regulation of organismal aging in response to mitochondrial dysfunction through multiple pathways.

Aging is also accompanied by various changes in mitochondria, including the decreased activity of mitochondrial enzymes, reduced mitochondrial oxygen consumption, increased ROS

production, decreased mitochondrial biogenesis, and increased mutations in mitochondrial DNA ²³⁻²⁷. Interestingly, different types and levels of mitochondrial DNA mutations accumulate in various tissues during aging in humans and model animals ^{28, 29}. Even within a single tissue, such as the brain and muscle, variations in mitochondrial DNA mutations have been reported ³⁰⁻³². As a result, there is growing interest in understanding how organisms respond to mitochondrial stress in specific tissues and cells.

Recent studies have elucidated the phenomenon wherein perturbations in mitochondrial function within a specific tissue can elicit lifespan extension and health improvement ^{16, 33, 34}. Remarkably, the nervous system exhibits a particular role in detecting its intrinsic mitochondrial stress and extending organismal lifespan ^{16, 33-36}. However, it remains unclear which neuronal subtype is responsible for extending organismal longevity in response to their mitochondrial stress and what mechanisms underlie the non-cell-autonomous changes in this regard.

γ-aminobutyric acid (GABA) is a widely utilized neurotransmitter found in both vertebrate and invertebrate nervous systems. In vertebrates, a substantial proportion, estimated to be between 30% and 40%, of central nervous system synapses rely on GABA transmission ³⁷. GABA levels tend to gradually decrease as organisms age, and disruptions in GABA neurotransmission have been associated with various neurological disorders and age-related cognitive decline ^{38, 39}. In *C. elegans*, 26 neurons have been anatomically and functionally characterized as GABAergic neurons ^{40, 41}. Interestingly, recent studies in *C. elegans* indicate that the GABA signaling pathway plays an important role in regulating the lifespan and overall health of the organism, mitochondrial unfolded protein response, and proteostasis in the post-synaptic muscle tissue ⁴²⁻⁴⁵.

In this study, we utilized C. elegans as a model organism to explore the role of GABAergic neurons in regulating organismal health and aging in response to mitochondrial perturbations, as well as the mechanisms underlying these effects. Our findings indicate that mitochondrial stress in GABAergic neurons can influence the activity of DAF-16/FoxO in peripheral tissues through

GABA signaling. This, in turn, leads to non-cell-autonomous alterations in the mitochondria activity and organismal healthspan, reproductive capacity, and lifespan.

Results

Mitochondrial perturbations in GABAergic neurons are sufficient to prolong the organismal lifespan

To explore the influence of mitochondrial dysfunction in GABAergic neurons on lifespan and healthspan, we inhibited the functions of *isp-1* and *spg-7*, well-documented genes that extend organismal lifespan when their normal functions are disrupted ^{11-13, 33, 46, 47}. In line with previous studies, systemic RNA interference (hereinafter referred to as sRNAi) targeting *isp-1* and *spg-7* significantly extended the lifespan of wild-type N2 animals when compared to control animals subjected to empty vector (EV) control RNAi (Figures 1A and 1B; Table S1). Tissue-specific RNAi in GABAergic neurons (hereinafter referred to as gRNAi) was accomplished by employing a previously well-established transgenic animal ⁴⁸⁻⁵⁰. In this model, the function of *rde-1*, a member of the PIWI/STING/Argonaute protein family, was specifically restored in GABAergic neurons by introducing a transgene that expresses RDE-1 under the control of the GABAergic neuron-specific promoter derived from the *unc-47* gene (Pgaba) (Figure 1C) ^{48, 51-53}. Additionally, they expressed *sid-1*, a gene responsible for dsRNA transport. When gRNAi against *isp-1* was induced from the L1 stage, it resulted in a median lifespan extension of 55.5% compared to the control (Figures 1D and Table S1). *spg-7(gRNAi)* animals also showed an extended median lifespan of 33.3% (Figure 1E and Table S1).

To exclude the possibility of any remaining systemic RNAi effects in the *rde-1* mutant background, we carried out another tissue-specific RNAi strategy ⁵⁴. We expressed *isp-1* double-stranded RNAs (dsRNAs) in GABAergic neurons using the Pgaba promoter (hereinafter referred to as *Pgaba::isp-1* dsRNA) in the *sid-1(qt9)* null mutant background, which lacks intercellular dsRNA transport, preventing sRNAi (Figure 1F) ^{55, 56}. The expression of *isp-1* dsRNAs in

GABAergic neurons within the wild-type N2 animal background proved effective in upregulating the expression of Phsp-6::GFP, which serves as a fluorescent reporter for mitoUPR activity, specifically in the intestine, suggesting that this *isp-1* dsRNA expression effectively induced mitochondrial defects (Figure S1A and S1B) ^{4, 34, 57}. Notably, we observed that Pgaba::isp-1 dsRNA expression in *sid-1* null mutants also significantly extended organismal lifespan (Figures 1G and Table S1) ⁵⁸⁻⁶⁰. Additionally, in 9-day-old adult *isp-1(gRNAi)* and *spg-7(gRNAi)* animals, we observed reduced lipofuscin fluorescence in the intestine, an aging hallmark that typically increases progressively over time (Figures 1H and 1I) ⁶¹. These findings collectively suggest that mitochondrial perturbation within GABAergic neurons is sufficient to prolong the organismal lifespan and attenuate the aging process.

Mitochondrial stress in GABAergic neurons increases the stress tolerance of the organism

Next, we sought to determine whether mitochondrial stress in GABAergic neurons could also alter the parameters of a healthspan. We tested thermal and oxidative stresses during aging, which are healthspan parameters closely linked to longevity across species ⁶²⁻⁶⁶ (Figure 2A). In mid-age adults (3-day-old adult) groups, gRNAi against *isp-1* and *spg-7* increased survivability against paraquat exposure compared to controls (Figure 2B). This improvement was also observed in older adult groups (Figures 2C and 2D). Moreover, *isp-1(gRNAi)* and *spg-7(gRNAi)* animals displayed a significant increase in survival when exposed to thermal stress at 35 °C (Figures 2E-2G). To validate the efficacy of RNAi, we maximized the RNAi effect by culturing animals under the feeding RNAi condition against *spg-7* for three generations (Figure S2A) and observed consistently improved survival rates in response to both oxidative stress (Figures S2B and S2C) and thermal stress (Figures S3D and S3E). In addition, *sid-1* null mutants expressing *Pgaba::isp-1* dsRNA expression also exhibited enhanced tolerance to thermal and paraquat stresses (Figures 2H and 2I). These findings suggest that mitochondrial stress in GABAergic neurons can enhance healthspan parameters.

GABAergic neuronal mitochondrial stress alters reproduction

143

144

145

146

147

148

149

150

151

152

153

154

155

156

157

158

159

160

161

162

163

164

165

166

167

168

While depletion of some mitochondrial ETC in the entire nervous system of C. elegans and flies increases lifespan in a non-cell-autonomous manner, it does not consistently affect fertility ^{8, 16}. Therefore, we sought to determine if mitochondrial dysfunction in GABAergic neurons similarly has no impact on reproduction. C. elegans exists as a hermaphrodite and produces a limited number of sperm in the L4 stage. In the adult stage, it undergoes oocyte development and self-fertilizes to produce embryos (Figure 3A) ^{67, 68}. While *isp-1* mutant has a prolonged lifespan, it has been shown to have a reduced brood size ⁶⁹. Interestingly, *isp-1* gRNAi was sufficient to reduce the number of fertile animals (Figure 3B). The total number of embryos produced by fertile isp-1(gRNAi) animals was also significantly decreased (P < 0.0001) (Figure 3C). When we assessed reproductive activity daily, fertile isp-1(gRNAi) animals displayed a reproductive period similar to that of the control group. However, brood sizes from the 2-day-old stage to the 4-dayold stage were significantly reduced (P<0.005 for the 2 and 3-day-old stages and P<0.0001 for the 4-day-old stage) (Figure 3D). Intrigued by these results, we evaluated the impact of isp-1(qRNAi) on the three critical stages of germline development including mitotic germ cell proliferation, meiotic germ cell apoptosis, and oogenesis (Figure 3A). Although the length of the mitotic area was not significantly affected by isp-1(gRNAi) (Figures 3E and S3A), the total number of mitotic germ cells was decreased during the early reproductive periods (1 to 3 days after the L4 stage) (Figure 3F). The number of apoptotic germ cells in the meiotic gonadal loop region, undergoing germline apoptosis, was not different from that in control animals at the 2-day-old adult stage, but it was substantially decreased at the 3-day-old stage (Figure 3G) 70. Thus, an increased loss of meiotic germ cells was not likely the primary cause of the reduced brood size. Interestingly, 2-day-old adult isp-1(gRNAi) animals displayed large DNA aggregates in the proximal gonad, a characteristic feature of an endomitotic oocyte phenotype (Figures 3H and 3I) ⁷¹. Once embryos were produced, most of them were hatched in *isp-1(qRNAi)* animals (Figure

S3B). Our results indicated that disruption of the mitochondrial ETC in GABAergic neurons negatively affected germline development and reproductive ability.

169

170

171

172

173

174

175

176

177

178

179

180

181

182

183

184

185

186

187

188

189

190

191

192

193

Mitochondrial stress in GABAergic neurons enhances mitochondrial function in the peripheral tissues

Accumulated evidence indicates that aging is linked to a decline in mitochondrial function and biogenesis ⁷²⁻⁷⁵. Additionally, experimentally increasing mitochondrial membrane potential and biogenesis is associated with lifespan extension 75,76. Therefore, we hypothesized that the mitochondrial stress specific to GABAergic neurons could impact the function and homeostasis of mitochondria in other peripheral tissues. At the 2-day-old stage, staining animals with the mitochondrial membrane potential-dependent MitoTracker Red CMXRos dye revealed a higher mitochondrial membrane potential in both the whole body (Figures 4A and 4B) and the intestine (Figure 4C) of isp-1(gRNAi) and spg-7(gRNAi) animals compared to that in the control group 77, ⁷⁸. Additionally, whole-body extracts from isp-1(qRNAi) animals showed a marked increase in ATP levels (Figure 4D). spg-7(gRNAi) animals showed somewhat higher ATP levels compared to the control group, but it was not significant (Figure 4D). Next, we stained isp-1(aRNAi) and spa-7(gRNAi) animals using the MitoTracker FM Green dye that accumulates in mitochondria in a membrane potential-independent manner, indicating the mass of mitochondria 79. We observed that both isp-1(gRNAi) and spg-7(gRNAi) animals exhibited higher MitoTracker FM Green fluorescence in the whole body than the control animals, suggesting an increase in mitochondrial mass (Figures 4E and 4F). In agreement with these results, the copy number of mitochondrial DNA was increased in isp-1(gRNAi) and spg-7(gRNAi) animals compared to control animals (Figure 4G). The expression of mitochondrial DNA polymerase gamma polg-1 was also significantly upregulated in isp-1(gRNAi) animals (Figure 4H) 35, 80, 81. Notably, staining isp-1(gRNAi) and spg-7(gRNAi) animals with the ROS indicator DCF-DA showed lower ROS levels

compared to the control animals (Figures 4I-4K) ⁸². Altogether, these results suggest that disturbances in mitochondrial homeostasis within GABAergic neurons could systemically increase overall mitochondrial membrane potential, ATP levels, and mitochondrial mass while decreasing ROS levels.

GABAergic neuronal Mitochondrial Stress Enhances the DAF-16/FoxO Pathway

194

195

196

197

198

199

200

201

202

203

204

205

206

207

208

209

210

211

212

213

214

215

216

217

218

219

Despite the increased total mitochondrial mass and activity, the decreased ROS levels in isp-1(aRNAi) and spa-7(aRNAi) animals suggest the possibility that their ability to mitigate oxidative stress has improved. Therefore, we analyzed changes in stress response regulators associated with mitochondria and ROS, including DAF-16/FoxO, mitoUPR, and SKN-1/Nrf ^{21, 57,} 83-85. It has been demonstrated that mutations in isp-1 and RNAi targeting isp-1 (isp-1 sRNAi) result in enhanced expression of reporter genes associated with the mitoUPR pathway, such as hsp-6 or hsp-60 4, 34, 57. In line with this, when the expression of Pgaba::isp-1 dsRNA was induced in N2 wild-type worms, leading to systemic isp-1 RNAi, a significant increase in Phsp-6::GFP expression was observed (Figures S1A and S1B). Additionally, we observed that sRNAi against isp-1 effectively triggered the expression of Phsp-6::GFP, and this induction was dependent on atfs-1, a crucial mediator of the mitoUPR pathway 86 (Figure S4A). These findings indicate the efficiency of our RNAi feeding conditions. However, isp-1 gRNAi did not significantly elevate the mRNA levels of hsp-60 and hsp-6, as evaluated by quantitative reverse transcription PCR (RTqPCR) analysis (Figure 5A). The mRNA level of qst-4, a downstream target of the SKN-1/Nrf pathway, was also not significantly increased by isp-1(gRNAi) (Figure 5A) 87, 88. In contrast, the mRNA levels of three DAF-16/FoxO downstream genes, including sod-3, hsp-16.2, and dlk-1, were substantially increased by isp-1(gRNAi) (Figure 5A) 89-91. Additionally, sid-1(eg9) null mutants expressing isp-1 dsRNA in GABAergic neurons also showed increased expression of DAF-16/FoxO target genes (Figure 5B). The intensity of a fluorescent reporter for the DAF-16/FoxO pathway (muls84 [Psod-3::gfp]) was also enhanced in this condition (Figures 5C and

5D). The elevated expression of *sod-3* and *dlk-1* induced by *isp-1(gRNAi)* was suppressed by the loss of DAF-16, suggesting that their expression is mediated by the DAF-16/FoxO pathway (Figure 5E).

220

221

222

223

224

225

226

227

228

229

230

231

232

233

234

235

236

237

238

239

240

241

242

243

244

245

The non-cell-autonomous effects of GABAergic neuronal mitochondrial defects require DAF-16/FoxO

Further investigations were conducted to evaluate the functional involvement of DAF-16/FoxO in the non-cell-autonomous effects of mitochondrial stress in GABAergic neurons. It was found that sRNAi against isp-1 required DAF-16/FoxO function to extend lifespan, as previously reported (Figure S4B and Table S1) ^{20, 21}. DAF-16/FoxO was also necessary for the enhanced tolerance against paraguat in isp-1(sRNAi) worms (Figure S4C). Notably, the lifespan extension by isp-1 gRNAi was suppressed in daf-16(mgDf47) null mutants (Figure 6A). Additionally, DAF-16/FoxO was required for the increased stress tolerance against thermal (Figure 6B) and paraquat (Figure 6C) stresses in isp-1(gRNAi) animals. DAF-16 loss also suppressed the upregulation of mitochondrial membrane potential (Figures 6D and 6E) and mitochondrial mass (Figures 6F and 6G) induced by isp-1 qRNAi. Moreover, qRNAi against isp-1 in the daf-16(mgDf47) null mutant background failed to increase mitochondrial DNA copy number (Figure 6H) and polg-1 mRNA levels (Figure 6I). Finally, the daf-16 null mutation suppressed the abnormalities in daily reproductive ability (Figure 6J) and total brood size (Figure 6K) caused by isp-1 gRNAi. Interestingly, the double RNAi knockdown of isp-1 and daf-16 in GABAergic neurons (isp-1+daf-16 qRNAi) also resulted in a normal lifespan, to a level similar to that displayed in EV(gRNAi) and daf-16(gRNAi) conditions, suggesting that DAF-16 function in GABAergic neurons is required to mediate the lifespan extension (Figure S4D and Table S1). These findings collectively suggest that DAF-16/FoxO plays a critical role in mediating non-cell autonomous changes resulting from GABAergic neuronal mitochondrial stress, influencing organismal lifespan, stress tolerance, mitochondrial homeostasis, and reproductive capacity.

Mitochondrial stress in GABAergic neurons causes non-cell-autonomous changes by acting on the same mechanisms as GABA signaling

Recent studies in *C. elegans* have revealed that GABA signaling plays a role not only in the regulation of GABAergic neuronal function but also in governing organismal longevity. Specifically, loss of *unc-25*, which encodes glutamic acid decarboxylase, has been shown to prolong lifespan and enhance stress tolerance ^{42, 43}. Hence, we conducted epistatic tests to investigate the possible interaction between the loss of GABA signaling and *isp-1* knockdown conditions in GABAergic neurons and their impact on organismal health and longevity. We found that targeting *isp-1* specifically in GABAergic neurons by expressing Pgaba::isp-1 dsRNAs in sid-1(qt9) mutants did not lead to a further extension of lifespan in *unc-25* null mutants (Figures 7A and S5A; Table S1). Additionally, GABAergic neuronal mitochondrial stress did not lead to an additive increase in stress tolerance beyond the levels observed in *unc-25(e156); sid-1(qt9)* mutants (Figures 7B and 7C). The enhanced GFP expression driven by the *sod-3* promoter due to *isp-1* dsRNA expression in GABAergic neurons was not further increased in the *unc-25* null mutant condition (Figure 7D).

Next, we assess if GABAergic neuronal mitochondrial stress affects GABA function by testing the sensitivity of animals to aldicarb, an acetylcholinesterase inhibitor that can cause post-synaptic receptor hyperstimulation and paralysis due to reduced acetylcholine breakdown ⁹². As previously reported, depletion of GABA in *unc-25* mutants increased the sensitivity to aldicarb ⁹² (Figures 7E). GABAergic neuronal expression of *isp-1* dsRNA also significantly elevated the sensitivity to aldicarb, particularly when animals were exposed to it for a prolonged period (120 min). The expression of *Pgaba::isp-1* dsRNA did not further increase the hypersensitivity to aldicarb in *unc-25* mutants, indicating that they function in the same pathway. Together, these findings suggest that diminished GABA signaling and mitochondrial stress within GABAergic neurons trigger alterations in organismal lifespan and healthspan through a common pathway.

Neuropeptide signaling in GABAergic neurons regulates organismal aging and health without additive effects with mitochondrial stress in GABAergic neurons

272

273

274

275

276

277

278

279

280

281

282

283

284

285

286

287

288

289

290

291

292

293

294

295

296

297

Next, we tested the potential roles of neuropeptide signaling in the non-cell autonomous effects of GABA neuronal mitochondrial stress 33. We measured the lifespan of mutants with mutations in *unc-31*, required for dense-core vesicle exocytosis ⁹⁵. In agreement with the previous report, unc-31(e928) mutants exhibited prolonged lifespan (Figure 8A and Table S1). There is no additive lifespan increase by Paaba::isp-1 dsRNA expression in the unc-31 mutant background. suggesting the potential involvement of neuropeptide signaling in regulating lifespan (Figure 8A and Table S1). GABAergic neurons have been suggested to express several neuropeptides, including flp-10, flp-11, flp-13, and flp-22 96,97. In line with previous studies, flp-13 was expressed in a subset of *C. elegans* GABAergic motor neurons (Figure S6A) ^{97, 98}. We found that *flp-13*+EV qRNAi extended the lifespan of animals compared to control animals, indicating its non-cell autonomous function in GABAergic neurons in regulating organismal lifespan (Figure 8B); Table S1). Double gRNAi against flp-13 and isp-1 did not further increase lifespan compared to flp-13+EV gRNAi alone, suggesting that depletion of FLP-13 and mitochondrial disruption in GABA neurons could extend lifespan through a common mechanism (Figure 8B and Table S1). While gRNAi against flp-13+EV did not affect the tolerance of animals against heat stress, it improved stress tolerance against paraguat to a level comparable to that observed in animals treated with flp-13+isp-1 double gRNAi (Figures 8C and 8D). Maximal treatment of flp-13 gRNAi, without mixing with EV bacteria, did not significantly increase the heat tolerance compared to the control group, suggesting that the lack of impact of flp-13+EV gRNAi on heat stress is unlikely to be attributed to a diluted RNAi efficiency due to the double RNAi method (Figure S6B). Additionally, maximal treatment of flp-13 gRNAi still showed enhanced paraguat tolerance and lifespan (Figures S6C and S6D; Table S1). Collectively, these findings indicate a novel role for the neuropeptide FLP-13 in regulating organismal aging and health. This regulation appears to be

mediated by a common mechanism associated with non-cell autonomous effects resulting from GABA neuronal mitochondrial dysfunction. The selective response of *flp-13* mutants to specific stressors implies the existence of additional mechanisms that respond to mitochondrial stress within GABAergic neurons.

Discussion

Our findings suggest that GABAergic neurons play a critical role in sensing mitochondrial stress and regulating longevity. Additionally, disrupting the mitochondria in GABAergic neurons alone was sufficient to induce alterations in organismal health and reproduction. Enhanced DAF-16/FoxO activity is necessary for mediating the non-cell autonomous changes observed in animals. Furthermore, we identified GABA signaling and one neuropeptide signaling as a factor associated with the non-cell autonomous effects caused by mitochondrial stress in GABAergic neurons.

Previous studies have demonstrated that mitochondrial stress in all neurons is sufficient to extend organismal lifespan. However, it remains incompletely understood which neurons respond to their mitochondrial stress to mediate this non-cell autonomous effects on organismal lifespan. Sha and colleagues have tested 18 neurons out of the total 302 in *C. elegans* regarding their potential to activate non-cell-autonomous effects and demonstrated that a specific subset, consisting of ASK, AWA, AWC, and AIA neurons, exhibits the capacity to induce non-cell-autonomous activation of the mitoUPR pathway in response to mitochondrial stress their mitochondria perturbation ³³. Interestingly, these conditions do not alter organismal lifespan, suggesting an unlink between mitoUPR and lifespan in certain conditions ³³.

The specific role of GABAergic neurons in non-cell autonomous regulation of aging and health in response to mitochondrial dysfunction has not been reported. This could be because these GABAergic neurons have not been tested or that previous studies primarily focused on neurons that non-cell autonomously affect the mitoUPR pathway in the peripheral tissues ^{16, 33-36}.

325

326

327

328

329

330

331

332

333

334

335

336

337

338

339

340

341

342

343

344

345

346

347

348

349

However, a recent study reveals that induced ROS production in GABAergic neurons can trigger mitoUPR induction in other peripheral tissues through activating UNC-49/GABAA receptor signaling, suggesting a central role of GABAergic neurons in regulating organismal stress response ⁴⁵. In our study, we prioritized monitoring changes in the lifespan rather than detecting mitoUPR reporter activity and found that inducing mitochondrial stress, specifically in GABAergic neurons, was sufficient to extend the lifespan of the animal. We employed two independent RNAi strategies to knock down two genes related to mitochondria. The tissue-specific RNAi approach, utilizing the rde-1(ne219) null mutant background and exclusively restoring rde-1 in target tissues, has been successfully utilized in multiple studies 48, 50, 51, 53. To eliminate the possibility of incomplete gRNAi, we also conducted isp-1 knockdown in GABAergic neurons by expressing isp-1 dsRNAs in sid-1 null mutant backgrounds, and we consistently observed an extension in lifespan in both RNAi strategies. isp-1 mutants and Pgaba::isp-1 dsRNA expression in wildtype animals robustly increase mitoUPR. In contrast, our gPCR results showed that there was no increase in mitoUPR reporter expression in *isp-1(gRNAi)* animals ⁴. Additionally, the *isp-1(gRNAi)* animals did not fully recapitulate the phenotypes of isp-1 mutants, including normal ATP level, increased ROS level, and decreased mitochondrial membrane potential 99-102, supporting that our two isp-1 knockdown conditions did not occur systemically other than in GABAergic neurons.

Longevity is associated with healthspan, but not in all cases ¹⁰³. Our results show that mitochondrial stress in GABAergic neurons not only prolonged lifespan but also improved stress tolerance, a typical healthspan parameter. Notably, we also found enhancements in mitochondria activity and ATP levels. These improvements in mitochondria could be, in part, a result of an increase in mitochondria population evidenced by increases in mitochondrial DNA copy number and mass. Consistently this notion, we also found increased mRNA levels of *polg-1*, encoding the mitochondrial DNA polymerase that is responsible for the replication of the mitochondrial genome, suggesting a potential increase in mitochondria biogenesis by GABAergic neuronal mitochondrial stress ^{35, 104}. The concept of aging in model organisms has long been linked to a decrease in

mitochondrial function and biogenesis ¹. Similarly, in humans, mitochondrial function declines with age ^{2, 105}. Enhancing mitochondrial function has been proposed as an intervention strategy against aging. In mice, the brain-specific overexpression of *Sirt1*, a pivotal regulator of mitochondrial biogenesis through PGC-1a, not only extended lifespan but also induced non-cell-autonomous effects in skeletal muscle including improved mitochondria homeostasis ⁷⁵. A recent study indicates that experimentally rejuvenated mitochondrial membrane potential is sufficient to extend *C. elegans* lifespan ⁷⁶. Additionally, while *isp-1* mutants have been shown to have elevated levels of ROS, a central factor in aging, our findings suggest that knockdown of *isp-1* in GABAergic neurons leads to a reduction in ROS levels, despite an increased mitochondrial population and heightened activity ^{6, 102, 106}. Therefore, both enhanced mitochondrial homeostasis and reduced ROS levels could contribute to the non-cell-autonomous enhancement in aging and health.

The reduced ROS also proposed the potential involvement of the stress response pathway against ROS. Strikingly, our qPCR results showed no evidence supporting the activation of mitoUPR by GABAergic-neuronal mitochondrial stress ^{16, 33-36}. It has been shown that *afts-1* acts cell-autonomously in certain neurons to mediate non-cell autonomous effects of mitochondrial stress in specific neurons ³³. Thus, it is still possible that mitoUPR activation in GABAergic neurons plays a role in mediating lifespan extension and improving stress resistance. Recent studies have demonstrated that experimentally enhanced ROS production in GABAergic neurons activates the mitoUPR and this requires UNC-49 GABA_A receptor ⁴⁵. However, *unc-49* mutants exhibit a normal lifespan ^{42, 43}. Therefore, the extended lifespan resulting from mitochondrial defects in GABAergic neurons is not primarily mediated by increased ROS production and noncell-autonomous activation of mitoUPR.

Our results suggested that GABAergic neuronal mitochondrial stress requires DAF-16/FoxO. We found that GABA-neuronal mitochondrial stress promoted the expression of *sod-3*, *hsp-16.2*, and *dlk-1*, which are regulated by DAF-16 ⁸⁹⁻⁹¹. A recent study also reveals that ROS induction in GABAergic neurons results in non-cell autonomously increased expression of *sod-3*

377

378

379

380

381

382

383

384

385

386

387

388

389

390

391

392

393

394

395

396

397

398

399

400

401

along with *hsp-6* ⁴⁵. DAF-16 is another pathway suggested to be activated by mitochondrial dysfunction, contributing to the extended lifespan observed in *C. elegans* with whole-body mitochondrial dysfunction ²¹. However, another study reports that while DAF-16 is required for the longevity of mitochondrial mutants in certain conditions, it was not sufficient to fully account for the observed lifespan extension ⁶. We found that depletion of DAF-16 suppressed a series of noncell-autonomous changes in lifespan, stress resistance, mitochondrial DNA (mtDNA) copy number, and *polg-1* expression. These results indicate the functional importance of DAF-16 in mediating the non-cell autonomous effects of mitochondrial disruption in GABAergic neurons.

Recent studies on C. elegans have reported that GABA signaling regulates lifespan and health 42, 43. Notably, GABA loss increases DAF-16/FoxO activity in the intestine, thereby increasing organismal longevity and health span 42, 43. Additionally, GABA signaling modulates protein homeostasis in C. elegans post-synaptic muscle cells 44. In contrast to the role of GABA signaling in C. elegans lifespan, knockdown of the Drosophila GABA_B receptor shorts lifespan ¹⁰⁷. Nevertheless, these results indicate that GABA signals could have a conserved role in regulating organismal health and aging. Our aldicarb assay results suggest that GABAergic neuronal mitochondrial stress could interfere with GABAergic neuronal activity. It has been revealed that mitochondria abundantly accumulate at the presynapse and affect synaptic activity by regulating the supply of ATP and calcium homeostasis, which are required for proper neurotransmitter release and recycling 108-113. Our previous studies have demonstrated that over 75% of mitochondria localize at the presynapse in GABAergic motor neurons in *C. elegans* ¹¹⁴. A screen for essential genes required for GABAergic neuronal function, utilizing a GABAergic neuronspecific feeding RNAi in C. elegans, has identified several mitochondrial-related genes. Knockdown of these genes in GABAergic neurons triggers hypersensitivity against aldicarb 48. Therefore, GABAergic neuronal mitochondrial perturbation could mimic effects induced by a reduction in GABA signaling. This hypothesis is supported by our epistatic analysis results, suggesting that GABAergic neuronal mitochondrial stress and the loss of GABA signaling in unc-

403

404

405

406

407

408

409

410

411

412

413

414

415

416

417

418

419

420

421

422

423

424

425

426

427

25 mutants may share a common mechanism influencing longevity, stress tolerance, and *sod-3* expression. Understanding how mitochondrial stress can modulate downstream mediators such as DAF-16 through altering GABA singling and ultimately affecting longevity and health can be complex. Mitochondrial stress in GABAergic neurons may partially reduce GABA signaling to varying degrees rather than completely turning it off ^{112, 115}. Moreover, GABA signaling differentially regulates lifespan and each healthspan parameter through three receptors and a combination of four downstream pathways ⁴³. Thus, reduced GABA signaling caused by GABA mitochondrial stress could affect each downstream receptor pathway to varying degrees, depending on the ability of each receptor to respond to GABA ligands.

It has been well-documented that cell-autonomous responses to mitochondrial defects can vary depending on the stressor conditions, including disruptions in each ETC component and disruption modes, pathological conditions, and environmental stressors 101, 116. These variations highlight the complex responses to mitochondrial disturbances. Interestingly, the non-cell autonomous longevity changes also differ depending on the type of mitochondrial perturbation. It has been reported that inhibition of spq-7 and cco-1, encoding a cytochrome c oxidase-1, in the entire nervous system prolongs lifespan ^{16, 33}, but it was not suppressed by mitoUPR loss. Mitochondrial stress induced by pan-neuronal expression of polyglutamine repeats (polyQ40) and mutation in ucp-4, encoding a mitochondrial uncoupling protein-4, do not further prolong the lifespan than wild-type animals, but mitoUPR function is required to preserve normal lifespan 33. Also, the deletion of spg-7 in AIY neurons is sufficient to induce mitoUPR in distal tissues but does not prolong lifespan ^{7,32,35}. Additionally, pan-neuronal expression of KillerRed, which induces oxidative stress, resulted in a reduced lifespan, despite an enhanced mitoUPR pathway in remote tissues ³³. In this study, we targeted to inhibition of *isp-1* and *spg-7* in GABAergic neurons and observed consistent changes in lifespan and stress resistance. Notably, isp-1 gRNAi resulted in decreased reproductive ability. Previous studies report that depletion of CCO-1, a component of mitochondria ETC, in the nervous system results in mitoUPR activation in the peripheral tissues

429

430

431

432

433

434

435

436

437

438

439

440

441

442

443

444

445

446

447

448

449

450

451

452

453

and prolongs lifespan without affecting brood size ^{16, 33}. Similarly, in *Drosophila*, ETC reduction in the nervous system increases longevity but maintains normal fertility ⁸. However, it remains unclear whether other mitochondrial stressors in GABAergic neurons can produce similar non-cell-autonomous effects as seen with *isp-1* and *spg-7* knockdown, which could be one reason the role of GABAergic neurons in regulating the non-cell-autonomous effects of mitochondrial disturbance has not been elucidated previously.

Finally, studies have demonstrated that neuropeptide signaling mediates the non-cell autonomous regulation of mitoUPR and organismal aging in response to mitochondrial stress in specific neurons ^{42, 117-122}. For instance, mitochondrial stress in ASK, AWA, AWC, and AIA neurons utilizes the FLP-2 neuropeptide to induce mitoUPR in peripheral tissues ³³. These results suggest that there could be additional signaling molecules mediating the non-cell autonomous effects of GABAergic neuronal mitochondrial stress. GABAergic neurons have been found to express several neuropeptides, including flp-10, flp-11, flp-13, and flp-22 96, 97. Our finding indicates that gRNAi against unc-31 increased lifespan resulting from depletion of dense core vesicle exocytosis was not further increased by GABA-neuronal mitochondrial stress, suggesting that neuropeptide signaling could be involved in non-autonomous changes caused by GABA-neuronal mitochondrial damage 95. FLP-13 loss increased lifespan and stress resistance, which is similar to the phenotype of animals with mitochondrial perturbations in GABAergic neurons. Animals with both conditions did show significant changes in stress resistance and lifespan compared to animals with either single condition, indicating that they work through the same mechanism to mediate non-cell autonomous effects. Therefore, it is possible that GABAergic neuronal mitochondrial stress reduces FLP-13 function, which inhibits lifespan and healthspan. Future studies are needed to elucidate the specific role of FLP-13 and other neuropeptides in the non-cellautonomous effects of GABA-neuronal mitochondrial stress.

Acknowledgment

We thank Drs. Shinichi Someya, Christiaan Leeuwenburgh, Stephanie Wohlgemuth, and Sejin Lee for their valuable discussions. Some strains were provided by the CGC, funded by the NIH Office of Research Infrastructure Programs (P40 OD010440). This research was conducted while SMH was a Hevolution/AFAR New Investigator Awardee in Aging Biology and Geroscience Research (AWD16056). SMH was also supported by the National Institute on Aging (NIA) of the National Institutes of Health (NIH) under award numbers R56AG066654 and R01AG081270, as well as the Glenn Foundation for Medical Research and the American Federation for Aging Research under award numbers AWD06577 and AWD11009 to SMH. Additionally, support was provided by NIA/NIH under award number AG060373-01 and the National Science Foundation under award number IOS (2132286) to MHL.

Author Contributions

S.M.H. supervised the study. M.H.L. and S.M.H. conceived the study. L.R. and S.M.H. wrote the manuscript with input from all authors. L.R. and S.C. designed and performed experiments and analyzed and interpreted data. Y. P. and M.H.L designed germline experiments and interpreted data. B.R. and T.M. assisted with planning and performing the stress response and lifespan assays. Y.S. and R.X generated reagents and assisted with planning and interpreting data. K.M., W.C., and R.X. provided expertise and resources and reviewed the manuscript.

Declaration of Interests

The authors declare no competing interests.

Inclusion and diversity

478 We support inclusive, diverse, and equitable conduct of research. 479 480 Data availability 481 All numerical data supporting the findings of this study are available in the supplemental 482 information and from the corresponding author upon reasonable request. 483 484 Material and Methods. 485 C. elegans strains 486 All C. elegans strains were maintained at 20 °C on nematode growth medium (NGM) plates 487 seeded with the OP50 strain of Escherichia coli (E. coli) as described before 123. A list of strains 488 used in this study is the following: N2 (Wild type), XE1375 (wpls36 l; wpSi1 ll; eri-1(mg366) IV; 489 rde-1(ne219) V; lin-15B(n744) X), SJ4100 (zcls13 [hsp-6p::gfp]), CB156 (unc-25(e156) III), 490 HC196 (sid-1(at9) V), GR1352 (daf-16(mqDf47)I), TJ356 (zIs356 IV [daf-16p::daf-16a/b::qfp; rol-491 6(su1006)]), CF1553 (muls84 [(pAD76) sod-3p::gfp + rol-6(su1006)]), CL2166 (dvls19 III 492 [(pAF15)gst-4p::gfp::NLS]). HAN260 (daf-16(mgDf47) I; wpls36 I; wpSi1 II; eri-1(mg366) IV; rde-493 1(ne219) V; lin-15B(n744) X), HAN186 (unc-25(e156); sid-1(qt9)), HAN356 (unc-25(e156); sid-494 1(at9)+sbsEx27 [unc-47p::isp-1 sense+ unc-47p::isp-1 antisense]), HAN357 (sid-495 1(qt9)+sbsEx27 [unc-47p::isp-1 sense+ unc-47p::isp-1 antisense]). 496 497 RNAi assay RNAi was performed by the feeding method ^{124, 125}. Briefly, freshly streaked single colonies of 498 499 HT115(DE3) bacteria containing either empty L4440 vector (control) or isp-1 and spg-7 RNAi 500 plasmid were grown overnight at 37 °C in Luria broth (LB) medium supplemented with carbenicillin 501 (25 μg/ml). HT115(DE3) bacterial feeding strains were obtained from the genome-wide library ¹²⁵. 502 PCR and sequencing were used to confirm that strains contained the correct clones. RNAi 503 bacteria were seeded on NGM plates containing IPTG (1 mM) and cultured overnight before

transferring animals. To prevent undesired non-specific effects, we did not use 5-fluoro-2'-deoxyuridine (FUdR) in seeded RNAi plates. Duplex RNAi was performed by mixing two HT115(DE3) bacterial strains, each containing the desired RNAi plasmid or empty vector in a 1:1 volume ratio. The efficiency of double RNAi, which involves feeding a 1:1 volume ratio mixture of bacteria strains targeting two different genes, was compared to that of single gene RNAi, which involves feeding a 1:1 volume ratio mixture of bacteria strains targeting one gene and an empty vector.

Lifespan assay

Age-synchronized animals were prepared by egg prep from adult animals cultured on each RNAi or regular NGM plate at 20°C ¹²⁶. The isolated embryos were transferred and allowed to hatch on RNAi NGM plates for the desired gene or regular NGM plates. Then, approximately 50 animals at the L4 stage were transferred to fresh RNAi plates. Every day, animals that failed to respond to gentle prodding with platinum wire were scored as dead. Lifespan data were statistically analyzed for significance by the log-rank test, comparing survival curves using GraphPad Prism software. Lifespan assays were performed at least in triplicate. To prevent undesired non-specific effects, we did not use 5-fluoro-2′-deoxyuridine (FUdR) in the seeded RNAi plates.

Aldicarb sensitivity assay

Aldicarb sensitivity assay was performed as described previously ⁹². Briefly, approximately 40-50 mutant animals were grown on OP50-seeded NGM plates at 20 °C for 72 hours. Approximately 40 L4 stage mutant animals were then picked and placed on 35 mm OP50-seeded NGM plates containing 0.5 mM aldicarb (Sigma Aldrich, 33386: prepared aldicarb NGM plates 1 day before the assay) and scored for paralysis every 30 minutes over a 120-minute period. Animals were considered paralyzed when they failed to show any movements in response to touching at a fixed time. This assay was carried out in triplicate for each experimental condition.

Reproductive assay

After pre-exposure to *spg-7* and *isp-1* RNAi from the L1 stage, age-synchronized XE1375 animals at the L4 stage (n=~20-30) were individually transferred to fresh *spg-7* and *isp-1* RNAi NGM plates. Every day, we moved mother animals to new *spg-7* and *isp-1* RNAi NGM plates until egg-laying stopped. The embryos produced daily were counted, and the total number of produced embryos was used to calculate the brood size. The egg production period was used to calculate the reproductive span, and the number of embryos produced each day was used to analyze reproductive trends. The hatching rate was scored 24 hours after egg-laying. The brood size, reproductive span, hatching rate, and reproductive trend data were generated from independent experiments. At least three replicate experiments were performed for each assay.

Stress assays

For the paraquat assay, 30-50 age-synchronized animals were pretreated to RNAi for each gene from the L1 stage. Then, 2-day-old adult animals were transferred to 96-well plates containing M9 with paraquat, a reactive oxygen species generator (Sigma-Aldrich, 36541-100MG), at a concentration of 0 mM, 50 mM, 100 mM, and 150 mM in a total volume of 100 µl per well. The survival of animals was evaluated after 24 hours, and animals that failed to respond to platinum wire touch were scored as dead. In the heat stress resistance assay, age-synchronized adult animals pretreated with *isp-1* or *spg-7* RNAi were exposed to thermal stress at 37°C for 5 hours. The survival after heat shock was recorded every hour for 5 hours by gently prodding with a platinum loop. Animals that failed to respond were scored as dead. All experiment was independently repeated at least three times.

Staining assays for ROS level and mitochondrial homeostasis

We used the fluorescent probe H₂DCF-DA dve (Invitrogen, D399) to detect ROS levels in vivo. as previously described 82. 2-day-old adult stage mutants or XE1375 animals pretreated with spg-7, isp-1, or control EV RNAi from the L1 stage were washed with M9 buffer to remove the bacteria. After washing 3 times, animals were collected in 300 µl of PTw buffer (1xPBS with 0.1% tween20). Then, around 30-35 animals were transferred to 96-well plates containing 10 mM H₂DCF-DA. The fluorescence was recorded using Spectra Max M2 multimode microplate reader (Molecular Devices) at 485 nm excitation and 530 nm emission. The change in fluorescence was recorded for 120 min at 20 min intervals at 37 °C. The experiment was performed 3 times independently. To perform the H₂DCF-DA assay using an image, we transferred 30-40 pretreated spg-7 and isp-1 RNAi animals in 500 µl M9 buffer and washed 3 times. Afterward, animals were incubated in 500 µl M9 buffer containing 10 mM H₂DCF-DA for 1 hour. Animals were washed with M9 buffer at least 3 times, transferred to 2% agarose pads on glass slides, and visualized using a GFP filter and imaged using a 40x objective (Andor, DSD2 spinning disk confocal, Andor, Zyra4.2 camera). To evaluate mitochondrial membrane potential and mass, we used MitoTracker CMXRos (Invitrogen, M7512) and FM green dye (Invitrogen, M7514), respectively, as described in previous studies ^{127, 128}. The lyophilized dyes were dissolved in DMSO and made to the final concentration of 100 μM. Animals were pretreated from the L1 stage to spg-7 and isp-1 gRNAi. L4 stage animals (n=30-40) were transferred to spg-7 and isp-1 RNAi plates with MitoTracker CMXRos or MitoTracker FM green dye and incubated for 48 hours at room temperature under dark conditions. Next, stained animals were transferred to fresh NGM plates (without the dye) for 1 hour to remove the bacterial fluorescent background inside the qut. The animals were observed using a 10x magnification to visualize the whole-body staining and a 40x objective to observe the anterior body, including the intestine.

ATP assay

555

556

557

558

559

560

561

562

563

564

565

566

567

568

569

570

571

572

573

574

575

576

577

578

579

We used previously reported protocols with a minor modification ⁵². Approximately 150 age-synchronized animals treated with *spg-7* and *isp-1* RNAi from the L1 stage were prepared.1-day-old adult animals were washed 5 times with M9 buffer to remove the intestinal bacteria and washed with TE buffer. The animals were frozen at -80 °C. The sample was sonicated for 15 seconds with a 15-second interval, followed by boiling for 10 minutes to release ATP and block ATPase activity. Debris was removed by centrifuging at 4 °C for 10 minutes. The supernatant was collected, and the ATP levels were measured using the bioluminescence detection kit (Promega ENLITEN ATP Assay System, FF2000) and Spectra Max M2 multimode microplate reader (Molecular Devices). Luminescence was normalized to protein content measured with a Pierce BCA protein determination kit (Thermo Scientific, 23227).

mtDNA quantification

580

581

582

583

584

585

586

587

588

589

590

591

592

593

594

595

596

597

598

599

600

601

602

603

604

605

mtDNA quantification was performed using a quantitative PCR (qPCR) based method ¹²⁹. About 30 age-synchronized L4 staged spg-7(gRNAi) and isp-1(gRNAi) animals were collected in 30 μl of lysis buffer (freshly added proteinase K) and frozen immediately at -80 °C for 10 minutes before lysis at 65 °C for 1 hour, followed by 95 °C for 15 minutes, and then maintained at 4 °C. Relative quantification was used for determining the fold changes in mtDNA. 2 µl of lysate sample was used as template DNA in each triplicate reaction. qPCR was performed using the SYBR green mixture in a CFX96 Touch Real-Time PCR System (Bio-Rad). Primers (mtDNA target-specific primer) for cox-4 and nd-1 were used to determine the mtDNA copy number. The cox-4 forward primer 5'GCCGACTGGAAGAACTTGTC-3' and reverse primer 5′-GCGGAGATCACCTTCCAGTA-3'. The nd-1 forward primer 5′-AGCGTCATTTATTGGGAAGAAGAC-3' 5′primer and reverse AAGCTTGTGCTAATCCCATAAATGT-3'. All qPCR results were performed in triplicates.

Quantitative reverse transcriptase PCR

RNA isolation and quantitative reverse transcriptase PCR (gRT-PCR) analysis were performed as previously described ¹³⁰. Animals raised on spg-7 or isp-1 gRNAi plates were synchronized by egg prep. Then, total RNA was extracted using the TRIzol (Invitrogen, 15596026) method from age-synchronized animals (approximately 1,500 animals at the 3-day-old adult stage). RNA was purified using a Qiagen Rneasy kit, and 2 µg RNA was used for cDNA synthesis (Thermo Scientific, Verso cDNA synthesis kit, AB1453A), qPCR was performed using SYBR Green master mix (Bio-Rad Laboratories). qPCR primers are listed below. Act-1 Forward 5′-5′-GCTGGACGTGATCTTACTGATTACC-3', act-1 Reverse GTAGCAGAGCTTCTCCTTGATGTC-3', daf-16 Forward 5'-CCAACACATTCATCCCAGTG-3', daf-16 5'-GATGGGATAGAGGTAGCATT-3', 5′-Reverse sod-3 Forward CTGATGGACACTATTAAGCG-3', sod-3 Reverse 5'-AAGTGGGACCATTCCTTCCAA-3', gst-5'-GCTGAGCCAATCCGTAT-3', gst-4 Reverse 5'-GTAAAATGGGAAGCTGGC-3′, dlk-1 Forward 5'-TCGACGCTATCTCCGAACTT-3'. dlk-1 Reverse 5′-TGCTTGATCTCGGTCTCCTT-3', hsp-6 Forward 5'-CGAAAGCTATTTGGGAACCA-3', hsp-6 5′-Reverse 5'-GCTCGTTGATGACACGAAGA-3', hsp-60 Forward CCGTCTCTGTCACTATGGGC-3', hsp-60 Reverse 5'-CTCGAATCCCTCTTTGGCGA-3', polq-1 Forward 5'-GTTACGGCCGACGAGATACG-3', polq-1 Reverse 5′-CGTAGCTTCCGGACTCCAAA-3'. All qPCR results were performed at least in triplicates.

Statistics

606

607

608

609

610

611

612

613

614

615

616

617

618

619

620

621

622

623

624

625

626

627

628

629

630

631

Statistics were performed using GraphPad PRISM (version 9 and 10). No statistical method was used to pre-determine sample size. For Figures 5D and 7D, outliers were identified using the ROUT method at Q = 1% and excluded from further analysis. Within experimental groups, animals were randomized for each experimental replicate. The qPCR experiments were analyzed using the delta-delta Ct method ¹²¹. All experiments were reliably reproduced at least 3 times independently. For the qPCR assays, in cases where the control and subjects were not paired,

the average control delta Ct value was utilized to calculate delta-delta Ct values. However, if the control and experimental groups were paired, individual control delta Ct values were used to

calculate delta-delta Ct values for each paired experimental group.

632

633

634

References

635

- 636 1. Rockstein, M. & Brandt, K.F. Enzyme changes in flight muscle correlated with aging and
- flight ability in the male housefly. *Science* **139**, 1049-1051 (1963).
- 638 2. Petersen, K.F. et al. Mitochondrial dysfunction in the elderly: possible role in insulin
- resistance. *Science* **300**, 1140-1142 (2003).
- 640 3. Dillin, A. et al. Rates of behavior and aging specified by mitochondrial function during
- development. *Science* **298**, 2398-2401 (2002).
- 642 4. Wu, Z. et al. Mitochondrial unfolded protein response transcription factor ATFS-1
- promotes longevity in a long-lived mitochondrial mutant through activation of stress
- response pathways. *BMC Biol* **16**, 147 (2018).
- 5. Felkai, S. et al. CLK-1 controls respiration, behavior and aging in the nematode
- 646 Caenorhabditis elegans. *Embo j* **18**, 1783-1792 (1999).
- 647 6. Feng, J., Bussière, F. & Hekimi, S. Mitochondrial electron transport is a key determinant
- of life span in Caenorhabditis elegans. *Dev Cell* **1**, 633-644 (2001).
- 649 7. Lee, S.S. et al. A systematic RNAi screen identifies a critical role for mitochondria in C.
- elegans longevity. *Nat Genet* **33**, 40-48 (2003).
- 651 8. Copeland, J.M. et al. Extension of Drosophila life span by RNAi of the mitochondrial
- 652 respiratory chain. *Curr Biol* **19**, 1591-1598 (2009).
- 653 9. Owusu-Ansah, E., Song, W. & Perrimon, N. Muscle mitohormesis promotes longevity via
- 654 systemic repression of insulin signaling. *Cell* **155**, 699-712 (2013).
- 655 10. Huang, X., Cheng, H.J., Tessier-Lavigne, M. & Jin, Y. MAX-1, a novel PH/MyTH4/FERM
- domain cytoplasmic protein implicated in netrin-mediated axon repulsion. Neuron **34**, 563-
- 657 576 (2002).
- 658 11. Chaudhari, S.N. & Kipreos, E.T. Increased mitochondrial fusion allows the survival of older
- animals in diverse C. elegans longevity pathways. *Nature communications* **8**, 182 (2017).

- 660 12. Maglioni, S., Mello, D.F., Schiavi, A., Meyer, J.N. & Ventura, N. Mitochondrial bioenergetic
- changes during development as an indicator of C. elegans health-span. *Aging (Albany*
- 662 NY) **11**, 6535-6554 (2019).
- 663 13. Chen, D., Pan, K.Z., Palter, J.E. & Kapahi, P. Longevity determined by developmental
- arrest genes in Caenorhabditis elegans. *Aging Cell* **6**, 525-533 (2007).
- 665 14. Ewbank, J.J. et al. Structural and functional conservation of the Caenorhabditis elegans
- timing gene clk-1. *Science* **275**, 980-983 (1997).
- 667 15. Liu, X. et al. Evolutionary conservation of the clk-1-dependent mechanism of longevity:
- loss of mclk1 increases cellular fitness and lifespan in mice. Genes Dev 19, 2424-2434
- 669 (2005).
- 670 16. Durieux, J., Wolff, S. & Dillin, A. The cell-non-autonomous nature of electron transport
- 671 chain-mediated longevity. *Cell* **144**, 79-91 (2011).
- 672 17. Bennett, C.F. et al. Activation of the mitochondrial unfolded protein response does not
- predict longevity in Caenorhabditis elegans. *Nature communications* **5**, 3483 (2014).
- 674 18. Tian, Y. et al. Mitochondrial Stress Induces Chromatin Reorganization to Promote
- 675 Longevity and UPR(mt). *Cell* **165**, 1197-1208 (2016).
- 676 19. Gao, K., Li, Y., Hu, S. & Liu, Y. SUMO peptidase ULP-4 regulates mitochondrial UPR-
- 677 mediated innate immunity and lifespan extension. *eLife* **8**, e41792 (2019).
- 678 20. Wolff, S. et al. SMK-1, an essential regulator of DAF-16-mediated longevity. Cell 124,
- 679 1039-1053 (2006).
- 680 21. Senchuk, M.M. et al. Activation of DAF-16/FOXO by reactive oxygen species contributes
- to longevity in long-lived mitochondrial mutants in Caenorhabditis elegans. PLoS Genet
- 682 **14**, e1007268 (2018).
- 683 22. Bennett, C.F. et al. Transaldolase inhibition impairs mitochondrial respiration and induces
- a starvation-like longevity response in Caenorhabditis elegans. *PLoS Genet* **13**, e1006695
- 685 (2017).

- 686 23. Cortopassi, G.A. & Arnheim, N. Detection of a specific mitochondrial DNA deletion in
- tissues of older humans. *Nucleic Acids Res* **18**, 6927-6933 (1990).
- 688 24. Pikó, L., Hougham, A.J. & Bulpitt, K.J. Studies of sequence heterogeneity of mitochondrial
- DNA from rat and mouse tissues: evidence for an increased frequency of
- 690 deletions/additions with aging. *Mech Ageing Dev* **43**, 279-293 (1988).
- 691 25. Hughes, A.L. & Gottschling, D.E. An early age increase in vacuolar pH limits mitochondrial
- 692 function and lifespan in yeast. *Nature* **492**, 261-265 (2012).
- 693 26. Hughes, C.E. et al. Cysteine Toxicity Drives Age-Related Mitochondrial Decline by Altering
- 694 Iron Homeostasis. *Cell* **180**, 296-310.e218 (2020).
- 695 27. Mansell, E. et al. Mitochondrial Potentiation Ameliorates Age-Related Heterogeneity in
- Hematopoietic Stem Cell Function. Cell Stem Cell 28, 241-256.e246 (2021).
- 697 28. Li, M., Schröder, R., Ni, S., Madea, B. & Stoneking, M. Extensive tissue-related and allele-
- related mtDNA heteroplasmy suggests positive selection for somatic mutations. *Proc Natl*
- 699 Acad Sci U S A **112**, 2491-2496 (2015).
- 700 29. Brandt, T. et al. Changes of mitochondrial ultrastructure and function during ageing in mice
- 701 and Drosophila. *Elife* **6** (2017).
- 702 30. Soong, N.W., Hinton, D.R., Cortopassi, G. & Arnheim, N. Mosaicism for a specific somatic
- 703 mitochondrial DNA mutation in adult human brain. *Nat Genet* **2**, 318-323 (1992).
- 704 31. Warren, C. et al. Decoding mitochondrial heterogeneity in single muscle fibres by imaging
- 705 mass cytometry. *Sci Rep* **10**, 15336 (2020).
- 706 32. Gredilla, R., Garm, C., Holm, R., Bohr, V.A. & Stevnsner, T. Differential age-related
- 707 changes in mitochondrial DNA repair activities in mouse brain regions. *Neurobiol Aging*
- 708 **31**, 993-1002 (2010).
- 709 33. Shao, L.W., Niu, R. & Liu, Y. Neuropeptide signals cell non-autonomous mitochondrial
- 710 unfolded protein response. Cell Res **26**, 1182-1196 (2016).

- 711 34. Zhang, Q. et al. The Mitochondrial Unfolded Protein Response Is Mediated Cell-Non-
- autonomously by Retromer-Dependent Wnt Signaling. Cell **174**, 870-883.e817 (2018).
- 713 35. Zhang, Q. et al. The memory of neuronal mitochondrial stress is inherited
- transgenerationally via elevated mitochondrial DNA levels. *Nat Cell Biol* **23**, 870-880
- 715 (2021).
- 716 36. Berendzen, K.M. et al. Neuroendocrine Coordination of Mitochondrial Stress Signaling
- 717 and Proteostasis. *Cell* **166**, 1553-1563.e1510 (2016).
- 718 37. Docherty, M., Bradford, H.F., Wu, J.Y., Joh, T.H. & Reis, D.J. Evidence for specific
- 719 immunolysis of nerve terminals using antisera against choline acetyltransferase,
- 720 glutamate decarboxylase and tyrosine hydroxylase. *Brain Res* **339**, 105-113 (1985).
- 721 38. McQuail, J.A., Frazier, C.J. & Bizon, J.L. Molecular aspects of age-related cognitive
- decline: the role of GABA signaling. *Trends Mol Med* **21**, 450-460 (2015).
- 723 39. Porges, E.C., Jensen, G., Foster, B., Edden, R.A. & Puts, N.A. The trajectory of cortical
- GABA across the lifespan, an individual participant data meta-analysis of edited MRS
- 725 studies. *Elife* **10** (2021).
- 726 40. Schuske, K., Beg, A.A. & Jorgensen, E.M. The GABA nervous system in C. elegans.
- 727 Trends Neurosci **27**, 407-414 (2004).
- 728 41. McIntire, S.L., Jorgensen, E., Kaplan, J. & Horvitz, H.R. The GABAergic nervous system
- 729 of Caenorhabditis elegans. *Nature* **364**, 337-341 (1993).
- 730 42. Chun, L. et al. Metabotropic GABA signalling modulates longevity in C. elegans. Nature
- 731 communications **6**, 8828 (2015).
- 732 43. Yuan, F. et al. GABA receptors differentially regulate life span and health span in C.
- elegans through distinct downstream mechanisms. Am J Physiol Cell Physiol 317, C953-
- 734 c963 (2019).

- 735 44. Garcia, S.M., Casanueva, M.O., Silva, M.C., Amaral, M.D. & Morimoto, R.I. Neuronal
- signaling modulates protein homeostasis in Caenorhabditis elegans post-synaptic muscle
- 737 cells. Genes Dev **21**, 3006-3016 (2007).
- 738 45. Pohl, F. et al. UNC-49 is a redox-sensitive GABA(A) receptor that regulates the
- 739 mitochondrial unfolded protein response cell nonautonomously. Sci Adv 9, eadh2584
- 740 (2023).
- 741 46. Van Raamsdonk, J.M. & Hekimi, S. Deletion of the mitochondrial superoxide dismutase
- sod-2 extends lifespan in Caenorhabditis elegans. *PLoS Genet* **5**, e1000361 (2009).
- 743 47. Feng, J., Bussière, F. & Hekimi, S. Mitochondrial electron transport is a key determinant
- of life span in Caenorhabditis elegans. *Developmental cell* **1**, 633-644 (2001).
- 745 48. Firnhaber, C. & Hammarlund, M. Neuron-specific feeding RNAi in C. elegans and its use
- in a screen for essential genes required for GABA neuron function. PLoS Genet 9,
- 747 e1003921 (2013).
- 748 49. Han, S.M., Baig, H.S. & Hammarlund, M. Mitochondria Localize to Injured Axons to
- 749 Support Regeneration. *Neuron* **92**, 1308-1323 (2016).
- 750 50. Qadota, H. et al. Establishment of a tissue-specific RNAi system in C. elegans. Gene 400.
- 751 166-173 (2007).
- 752 51. Timmons, L. & Fire, A. Specific interference by ingested dsRNA. *Nature* **395**, 854 (1998).
- 753 52. Han, S.M. et al. VAPB/ALS8 MSP ligands regulate striated muscle energy metabolism
- critical for adult survival in caenorhabditis elegans. *PLoS Genet* **9**, e1003738 (2013).
- 755 53. Zou, L. et al. Construction of a germline-specific RNAi tool in C. elegans. Sci Rep 9, 2354
- 756 (2019).
- 757 54. Calixto, A., Chelur, D., Topalidou, I., Chen, X. & Chalfie, M. Enhanced neuronal RNAi in
- 758 C. elegans using SID-1. *Nat Methods* **7**, 554-559 (2010).

- 759 55. Tavernarakis, N. & Driscoll, M. Caenorhabditis elegans degenerins and vertebrate ENaC
- ion channels contain an extracellular domain related to venom neurotoxins. *J Neurogenet*
- 761 **13**, 257-264 (2000).
- 762 56. Tabara, H. et al. The rde-1 gene, RNA interference, and transposon silencing in C.
- 763 elegans. *Cell* **99**, 123-132 (1999).
- 764 57. Yoneda, T. et al. Compartment-specific perturbation of protein handling activates genes
- encoding mitochondrial chaperones. *J Cell Sci* **117**, 4055-4066 (2004).
- 766 58. Shih, J.D. & Hunter, C.P. SID-1 is a dsRNA-selective dsRNA-gated channel. *Rna* 17,
- 767 1057-1065 (2011).
- Feinberg, E.H. & Hunter, C.P. Transport of dsRNA into cells by the transmembrane protein
- 769 SID-1. Science **301**, 1545-1547 (2003).
- 770 60. Winston, W.M., Molodowitch, C. & Hunter, C.P. Systemic RNAi in C. elegans requires the
- putative transmembrane protein SID-1. Science **295**, 2456-2459 (2002).
- 772 61. Garigan, D. et al. Genetic analysis of tissue aging in Caenorhabditis elegans: a role for
- heat-shock factor and bacterial proliferation. *Genetics* **161**, 1101-1112 (2002).
- 1774 62. Lithgow, G.J., White, T.M., Melov, S. & Johnson, T.E. Thermotolerance and extended life-
- span conferred by single-gene mutations and induced by thermal stress. *Proc Natl Acad*
- 776 Sci U S A **92**, 7540-7544 (1995).
- 777 63. Harshman, L.G. & Haberer, B.A. Oxidative stress resistance: a robust correlated response
- 778 to selection in extended longevity lines of Drosophila melanogaster? J Gerontol A Biol Sci
- 779 *Med Sci* **55**, B415-417 (2000).
- 780 64. Fabrizio, P., Pozza, F., Pletcher, S.D., Gendron, C.M. & Longo, V.D. Regulation of
- longevity and stress resistance by Sch9 in yeast. Science **292**, 288-290 (2001).
- 782 65. Johnson, T.E. et al. Longevity genes in the nematode Caenorhabditis elegans also
- 783 mediate increased resistance to stress and prevent disease. J Inherit Metab Dis 25, 197-
- 784 206 (2002).

- 785 66. Murakami, S., Salmon, A. & Miller, R.A. Multiplex stress resistance in cells from long-lived
- 786 dwarf mice. *FASEB J* **17**, 1565-1566 (2003).
- 787 67. Kimble, J. & Seidel, H. C. elegans germline stem cells and their niche, in *StemBook*
- 788 (Harvard Stem Cell Institute
- 789 Copyright: © 2013 Judith Kimble and Hannah Seidel., Cambridge (MA); 2008).
- 790 68. Hubbard, E.J. & Greenstein, D. Introduction to the germ line. *WormBook*, 1-4 (2005).
- 791 69. Dues, D.J. et al. Uncoupling of oxidative stress resistance and lifespan in long-lived isp-1
- mitochondrial mutants in Caenorhabditis elegans. Free Radic Biol Med 108, 362-373
- 793 (2017).
- 794 70. Gumienny, T.L., Lambie, E., Hartwieg, E., Horvitz, H.R. & Hengartner, M.O. Genetic
- control of programmed cell death in the Caenorhabditis elegans hermaphrodite germline.
- 796 Development **126**, 1011-1022 (1999).
- 797 71. Clandinin, T.R., DeModena, J.A. & Sternberg, P.W. Inositol trisphosphate mediates a
- 798 RAS-independent response to LET-23 receptor tyrosine kinase activation in C. elegans.
- 799 *Cell* **92**, 523-533 (1998).
- 800 72. Marcus, D.L., Ibrahim, N.G. & Freedman, M.L. Age-related decline in the biosynthesis of
- mitochondrial inner membrane proteins. *Exp Gerontol* **17**, 333-341 (1982).
- 802 73. Bailey, P.J. & Webster, G.C. Lowered rates of protein synthesis by mitochondria isolated
- from organisms of increasing age. *Mech Ageing Dev* **24**, 233-241 (1984).
- 804 74. Rooyackers, O.E., Adey, D.B., Ades, P.A. & Nair, K.S. Effect of age on in vivo rates of
- 805 mitochondrial protein synthesis in human skeletal muscle. *Proc Natl Acad Sci U S A* **93**,
- 806 15364-15369 (1996).
- 807 75. Satoh, A. et al. Sirt1 Extends Life Span and Delays Aging in Mice through the Regulation
- 808 of Nk2 Homeobox 1 in the DMH and LH. Cell Metabolism 18, 416-430 (2013).

- 809 76. Berry, B.J. et al. Optogenetic rejuvenation of mitochondrial membrane potential extends
- 810 C. elegans lifespan. *Nature Aging* **3**, 157-161 (2023).
- 77. Pendergrass, W., Wolf, N. & Poot, M. Efficacy of MitoTracker Green and CMXrosamine
- to measure changes in mitochondrial membrane potentials in living cells and tissues.
- 813 Cytometry A **61**, 162-169 (2004).
- 814 78. Han, S.M. et al. Secreted VAPB/ALS8 major sperm protein domains modulate
- mitochondrial localization and morphology via growth cone guidance receptors. Dev Cell
- 816 **22**, 348-362 (2012).
- 817 79. Monteiro, L.B., Davanzo, G.G., de Aguiar, C.F. & Moraes-Vieira, P.M.M. Using flow
- cytometry for mitochondrial assays. *MethodsX* **7**, 100938 (2020).
- 819 80. Bratic, I. et al. Mitochondrial DNA level, but not active replicase, is essential for
- Caenorhabditis elegans development. *Nucleic Acids Res* **37**, 1817-1828 (2009).
- 821 81. Gui, Y.X., Xu, Z.P., Lv, W., Zhao, J.J. & Hu, X.Y. Evidence for polymerase gamma, POLG1
- variation in reduced mitochondrial DNA copy number in Parkinson's disease.
- 823 Parkinsonism Relat Disord **21**, 282-286 (2015).
- 824 82. Yoon, D.S., Lee, M.H. & Cha, D.S. Measurement of Intracellular ROS in Caenorhabditis
- 825 elegans Using 2',7'-Dichlorodihydrofluorescein Diacetate. *Bio Protoc* **8** (2018).
- 826 83. Blackwell, T.K., Steinbaugh, M.J., Hourihan, J.M., Ewald, C.Y. & Isik, M. SKN-1/Nrf, stress
- responses, and aging in Caenorhabditis elegans. Free Radic Biol Med 88, 290-301 (2015).
- 828 84. Haynes, C.M., Petrova, K., Benedetti, C., Yang, Y. & Ron, D. ClpP mediates activation of
- 829 a mitochondrial unfolded protein response in C. elegans. Dev Cell 13, 467-480 (2007).
- 830 85. Haynes, C.M., Fiorese, C.J. & Lin, Y.F. Evaluating and responding to mitochondrial
- dysfunction: the mitochondrial unfolded-protein response and beyond. *Trends Cell Biol*
- 832 **23**, 311-318 (2013).

- 833 86. Nargund, A.M., Pellegrino, M.W., Fiorese, C.J., Baker, B.M. & Haynes, C.M. Mitochondrial
- import efficiency of ATFS-1 regulates mitochondrial UPR activation. Science 337, 587-
- 835 590 (2012).
- 836 87. Leiers, B. et al. A stress-responsive glutathione S-transferase confers resistance to
- 837 oxidative stress in Caenorhabditis elegans. Free Radic Biol Med **34**, 1405-1415 (2003).
- 838 88. Wang, J. et al. RNAi screening implicates a SKN-1-dependent transcriptional response in
- stress resistance and longevity deriving from translation inhibition. *PLoS Genet* **6** (2010).
- 840 89. Byrne, A.B. et al. Insulin/IGF1 signaling inhibits age-dependent axon regeneration.
- 841 Neuron **81**, 561-573 (2014).
- 842 90. Honda, Y. & Honda, S. The daf-2 gene network for longevity regulates oxidative stress
- resistance and Mn-superoxide dismutase gene expression in Caenorhabditis elegans.
- 844 Faseb j **13**, 1385-1393 (1999).
- 845 91. Libina, N., Berman, J.R. & Kenyon, C. Tissue-specific activities of C. elegans DAF-16 in
- the regulation of lifespan. *Cell* **115**, 489-502 (2003).
- 847 92. Mahoney, T.R., Luo, S. & Nonet, M.L. Analysis of synaptic transmission in Caenorhabditis
- 848 elegans using an aldicarb-sensitivity assay. *Nat Protoc* **1**, 1772-1777 (2006).
- 849 93. Jin, Y., Jorgensen, E., Hartwieg, E. & Horvitz, H.R. The Caenorhabditis elegans gene unc-
- 850 25 encodes glutamic acid decarboxylase and is required for synaptic transmission but not
- 851 synaptic development. *J Neurosci* **19**, 539-548 (1999).
- 852 94. Vashlishan, A.B. et al. An RNAi screen identifies genes that regulate GABA synapses.
- 853 Neuron **58**, 346-361 (2008).
- 854 95. Speese, S. et al. UNC-31 (CAPS) is required for dense-core vesicle but not synaptic
- vesicle exocytosis in Caenorhabditis elegans. *J Neurosci* **27**, 6150-6162 (2007).
- 856 96. Li, C. & Kim, K. Neuropeptides. *WormBook*, 1-36 (2008).

- 857 97. Melkman, T. & Sengupta, P. Regulation of chemosensory and GABAergic motor neuron
- development by the C. elegans Aristaless/Arx homolog alr-1. *Development* **132**, 1935-
- 859 1949 (2005).
- 860 98. Shan, G., Kim, K., Li, C. & Walthall, W.W. Convergent genetic programs regulate
- 861 similarities and differences between related motor neuron classes in Caenorhabditis
- 862 elegans. *Developmental Biology* **280**, 494-503 (2005).
- 99. Jafari, G. *et al.* Tether mutations that restore function and suppress pleiotropic phenotypes
- of the C. elegans isp-1(qm150) Rieske iron-sulfur protein. *Proc Natl Acad Sci U S A* **112**,
- 865 E6148-6157 (2015).
- 100. Lemire, B.D., Behrendt, M., DeCorby, A. & Gášková, D. C. elegans longevity pathways
- 867 converge to decrease mitochondrial membrane potential. *Mechanisms of Ageing and*
- 868 Development **130**, 461-465 (2009).
- 869 101. Yang, W. & Hekimi, S. Two modes of mitochondrial dysfunction lead independently to
- lifespan extension in Caenorhabditis elegans. *Aging Cell* **9**, 433-447 (2010).
- 871 102. Lee, S.J., Hwang, A.B. & Kenyon, C. Inhibition of respiration extends C. elegans life span
- via reactive oxygen species that increase HIF-1 activity. *Curr Biol* **20**, 2131-2136 (2010).
- 873 103. Bansal, A., Zhu, L.J., Yen, K. & Tissenbaum, H.A. Uncoupling lifespan and healthspan in
- 874 Caenorhabditis elegans longevity mutants. *Proc Natl Acad Sci U S A* **112**, E277-286
- 875 (2015).
- 876 104. Rahman, S. & Copeland, W.C. POLG-related disorders and their neurological
- 877 manifestations. *Nat Rev Neurol* **15**, 40-52 (2019).
- 878 105. Short, K.R. et al. Decline in skeletal muscle mitochondrial function with aging in humans.
- 879 *Proc Natl Acad Sci U S A* **102**, 5618-5623 (2005).
- 880 106. Back, P., Braeckman, B.P. & Matthijssens, F. ROS in aging Caenorhabditis elegans:
- damage or signaling? Oxid Med Cell Longev 2012, 608478 (2012).

- 882 107. Enell, L.E., Kapan, N., Söderberg, J.A., Kahsai, L. & Nässel, D.R. Insulin signaling,
- lifespan and stress resistance are modulated by metabotropic GABA receptors on insulin
- producing cells in the brain of Drosophila. *PLoS One* **5**, e15780 (2010).
- 108. Ly, C.V. & Verstreken, P. Mitochondria at the synapse. *Neuroscientist* **12**, 291-299 (2006).
- 886 109. Kwon, S.K. et al. LKB1 Regulates Mitochondria-Dependent Presynaptic Calcium
- 887 Clearance and Neurotransmitter Release Properties at Excitatory Synapses along Cortical
- 888 Axons. *PLoS Biol* **14**, e1002516 (2016).
- 889 110. Sun, T., Qiao, H., Pan, P.Y., Chen, Y. & Sheng, Z.H. Motile axonal mitochondria contribute
- to the variability of presynaptic strength. *Cell reports* **4**, 413-419 (2013).
- 891 111. Ivannikov, M.V., Sugimori, M. & Llinas, R.R. Synaptic vesicle exocytosis in hippocampal
- 892 synaptosomes correlates directly with total mitochondrial volume. *J Mol Neurosci* **49**, 223-
- 893 230 (2013).
- 894 112. Verstreken, P. et al. Synaptic mitochondria are critical for mobilization of reserve pool
- vesicles at Drosophila neuromuscular junctions. *Neuron* **47**, 365-378 (2005).
- 896 113. Smith, H.L. et al. Mitochondrial support of persistent presynaptic vesicle mobilization with
- 897 age-dependent synaptic growth after LTP. *Elife* **5** (2016).
- 898 114. Schultz, J. et al. The secreted MSP domain of C. elegans VAPB homolog VPR-1 patterns
- the adult striated muscle mitochondrial reticulum via SMN-1. Development 144, 2175-
- 900 2186 (2017).
- 901 115. Sun, T., Qiao, H., Pan, P.Y., Chen, Y. & Sheng, Z.H. Motile axonal mitochondria contribute
- to the variability of presynaptic strength. *Cell Rep* **4**, 413-419 (2013).
- 903 116. Gorman, G.S. et al. Mitochondrial diseases. Nat Rev Dis Primers 2, 16080 (2016).
- 904 117. Jeong, D.E., Artan, M., Seo, K. & Lee, S.J. Regulation of lifespan by chemosensory and
- thermosensory systems: findings in invertebrates and their implications in mammalian
- 906 aging. Front Genet **3**, 218 (2012).

- 907 118. Wolkow, C.A., Kimura, K.D., Lee, M.S. & Ruvkun, G. Regulation of C. elegans life-span
- by insulinlike signaling in the nervous system. *Science* **290**, 147-150 (2000).
- 909 119. Taguchi, A., Wartschow, L.M. & White, M.F. Brain IRS2 signaling coordinates life span
- 910 and nutrient homeostasis. *Science* **317**, 369-372 (2007).
- 911 120. Apfeld, J. & Kenyon, C. Regulation of lifespan by sensory perception in Caenorhabditis
- 912 elegans. *Nature* **402**, 804-809 (1999).
- 913 121. Alcedo, J. & Kenyon, C. Regulation of C. elegans longevity by specific gustatory and
- 914 olfactory neurons. *Neuron* **41**, 45-55 (2004).
- 915 122. Chen, Y.C. et al. A C. elegans Thermosensory Circuit Regulates Longevity through crh-
- 916 1/CREB-Dependent flp-6 Neuropeptide Signaling. Dev Cell 39, 209-223 (2016).
- 917 123. Brenner, S. The genetics of Caenorhabditis elegans. *Genetics* **77**, 71-94 (1974).
- 918 124. Kamath, R.S., Martinez-Campos, M., Zipperlen, P., Fraser, A.G. & Ahringer, J.
- 919 Effectiveness of specific RNA-mediated interference through ingested double-stranded
- 920 RNA in Caenorhabditis elegans. *Genome Biol* **2**, RESEARCH0002 (2001).
- 921 125. Kamath, R.S. & Ahringer, J. Genome-wide RNAi screening in Caenorhabditis elegans.
- 922 Methods **30**, 313-321 (2003).
- 923 126. Stiernagle, T. Maintenance of C. elegans. WormBook, 1-11 (2006).
- 924 127. Han, S.M. et al. Deleted in cancer 1 (DICE1) is an essential protein controlling the topology
- of the inner mitochondrial membrane in C. elegans. *Development* **133**, 3597-3606 (2006).
- 926 128. Dingley, S. et al. Mitochondrial respiratory chain dysfunction variably increases oxidant
- 927 stress in Caenorhabditis elegans. *Mitochondrion* **10**, 125-136 (2010).
- 928 129. Rooney, J.P. et al. PCR based determination of mitochondrial DNA copy number in
- 929 multiple species. *Methods Mol Biol* **1241**, 23-38 (2015).
- 930 130. Sheng, Y., Yang, G., Markovich, Z., Han, S.M. & Xiao, R. Distinct temporal actions of
- different types of unfolded protein responses during aging. *J Cell Physiol* **236**, 5069-5079
- 932 (2021).

933 131. Grishok, A., Tabara, H. & Mello, C.C. Genetic requirements for inheritance of RNAi in C. elegans. *Science* **287**, 2494-2497 (2000).

935

936

937

132. Wang, D. *et al.* Somatic misexpression of germline P granules and enhanced RNA interference in retinoblastoma pathway mutants. *Nature* **436**, 593-597 (2005).

Figure Legend

Figure 1. Mitochondrial stress in GABAergic neurons is sufficient to prolong the organismal lifespan.

(A and B) Lifespan analysis of systemic isp-1(sRNAi) and spg-7(sRNAi) animals. (C) GABAneuron-specific RNAi system. The gRNAi system is based on the rde-1 mosaic mutant background, which carries a loss-of-function mutation in rde-1, thereby preventing RNAi 48, 50, 51, ^{53, 56, 131}. This system also involves *eri-1* and *lin-15* loss-of-function mutant backgrounds, resulting in hyperactivated RNAi sensitivity in all neurons 48, 132. Restricted feeding RNAi to GABAergic neurons is achieved by exclusive RDE-1 expression in GABAergic neurons, along with the SID-1 dsRNA channel protein ⁴⁸. (D and E) Lifespan analysis of isp-1(gRNAi) and spg-7(gRNAi) animals. (F) GABAergic neuron-specific isp-1 RNAi through in vivo transcription of sense and antisense RNAs in GABAergic neurons under the sid-1(eq9) null mutant background. (G) Lifespan analysis of sid-1(at9) and sid-1(at9)+Paba::isp-1 dsRNA animals. The significance of the lifespan curves (A, B, D, E, and G) was assessed using a Log-rank (Mantel-Cox) test. (H and I) The levels of lipofuscin in isp-1(gRNAi) and spg-7(gRNAi) animals at the 9-day-old adult stage were compared to those in control animals. (H) Representative images of lipofuscin fluorescence in the whole body of animals under the indicated conditions. Bar, 50 µm. (I) Quantification of lipofuscin fluorescence intensity. Each dot represents a single animal. ****P < 0.0001; one-way ANOVA test. Data are expressed as means ± SEM. Created with https://www.biorender.com/.

Figure 2. Mitochondrial stress in GABAergic neurons enhances stress resistance

(A) A diagram illustrating the paraquat and thermal stress experimental procedures is provided. (B-D) The survival rate of animals cultured in indicated concentrations of paraquat for 24 hours was measured at 3, 6, and 9-day-old adult stages. (E-G) The survival rate after incubation at 35°C for 5 hours was measured in animals at 3, 6, and 9-day-old adult stages. At least 30 animals were tested for each set. Statistical significance is indicated as follows: (H-I) Survival rates of animals

at the 3-day-old adult stage after 100 mM paraquat treatment for 24 hours (H) and 24 hours after incubation at 35°C for 5 hours (I) were measured. *P < 0.05, **P < 0.005, ***P < 0.0005, ***P < 0.0001; one-way ANOVA test. Data are expressed as means \pm SEM.

Figure 3. Reproductive effects of mitochondrial perturbation in GABAergic neurons.

(A) A diagram of the C. elegans hermaphrodite reproductive system was presented, showing the distal gonad with the mitotic area for germ cell proliferation, the meiotic germ area for meiosis, and an area undergoing germ cell apoptosis, the proximal area with oogenesis, the spermatheca for sperm storage, and the uterus for fertilized egg storage. (B) Sterility in isp-1(gRNAi) animals compared to control animals. (C) The total number of embryos in fertile isp-1(qRNAi) and spq-7(gRNAi) animals. (D) The daily brood size in fertile isp-1(gRNAi) and spg-7(gRNAi) animals. (E) Representative images of dissected distal gonad arms stained with DAPI from 2-day-old isp-1(qRNAi) and control animals. The dashed lines indicate the endpoint of the mitotic area. (F) Quantitative analysis of germ cell numbers in the mitotic regions of isp-1(gRNAi) and control animals. (G) A violin plot is presented, displaying the median (solid line) and quartiles (dashed lines), illustrating the apoptotic germ cells in the loop regions of isp-1(gRNAi) and control animals. (H) Representative images of dissected proximal gonad stained with DAPI from 2-day-old isp-1(gRNAi) and control animals. The arrowheads indicate stained oocyte chromosomes. (I) Quantitative analysis of endomitotic nuclei in diakinesis oocytes in the proximal gonad of isp-1(gRNAi) and control animals. Statistical significance is indicated as follows: *P < 0.05, ***P < 0.0005, ****P < 0.0001; two-tailed Mann-Whitney test. Each dot represents an individual worm (C and D) and gonad arm (F, G, and I). Additionally, each dot indicates an individual group (B and I), animal (C and D), and gonad (F and G). Data are expressed as means ± SEM except (G). Created with https://www.biorender.com/.

Figure 4. GABAergic neuronal mitochondrial stress alters the mitochondrial homeostasis

in peripheral tissues of animals.

expressed as means ± SEM. Bars, 50 µm.

(A) Representative images of mitochondrial membrane potential in isp-1(gRNAi) and spg-7(gRNAi) animals after MitoTracker CMXRos dye staining at 3-day-old adults. (B and C) Quantitative analysis of MitoTracker CMXRos fluorescent intensity measured by microscopy with a 100x magnification in the indicated animals at 3-day-old adult stage (B) and in the anterior intestine region assessed by microscopy with a 400x magnification (C). (D) The ATP bioluminescence assay measured ATP levels in the whole-body extracts of isp-1(gRNAi) and spg-7(gRNAi) animals. (E) Representative image of MitoTracker FM Green fluorescence in animals at 3-day-old adults to visualize mitochondrial mass. (F) Quantitative MitoTracker FM Green fluorescence intensity in isp-1(gRNAi) and spg-7(gRNAi) animals (G) Relative mtDNA copy number analyzed by the qPCR method in isp-1(qRNAi) and spq-7(qRNAi) animals. (H) Relative transcript levels of mitochondrial DNA polymerase gamma polq-1 gene expression measured by qPCR in isp-1(qRNAi) animals at the 2-day-old adult stage. (I) Representative images of isp-1(gRNAi) and spg-7(gRNAi) animals stained with H2DCF-DA dye to measure ROS levels in the whole body. (J) Quantitative analysis of H2DCF fluorescent intensity monitored by a spectrophotometer in isp-1(gRNAi) and spg-7(gRNAi) animals at 3-day-old adults. (K) Quantitative fluorescence intensity in the anterior intestine of animals after H2DCF-DA staining with a 400x magnification. Statistical significance is indicated as follows: *P < 0.05, **P < 0.005, ***P < 0.0005, ****P < 0.0001; one-way ANOVA test for (B, C, D, F, G, J, and K) and two-tailed student's t-test for (H). Each dot indicates an individual worm (B, C, F, J, and K). Data are

Figure 5. GABAergic neuronal mitochondria stress elevated the DAF-16/FoxO pathway.

(A) RT-qPCR analysis to assess the relative transcript levels of mitoUPR, SKN-1/Nrf, and DAF-16/FoxO signaling target genes in isp-1(gRNAi) animals compared to control EV(gRNAi) animals. The expression levels of each gene were normalized to the reference gene act-2 which encodes actin. (B) RT-qPCR analysis was conducted to assess the relative transcript levels of sod-3 in sid-1(qt9) null mutants expressing isp-1 dsRNA in GABAergic neurons. (C and D) Representative images and the quantification of Psod-3::GFP expression, a reporter for DAF-16/FoxO activity, in sid-1(qt9) control animals and sid-1(qt9)+Pgaba::isp-1 dsRNA animals. Each dot indicates an individual worm. (E) RT-qPCR analysis was performed to assess the relative transcript levels of sod-3 and dlk-1 in daf-16(mgDf47) null mutants, both with and without isp-1 gRNAi treatment. Statistical significance is indicated as follows: **P < 0.005, ***P < 0.0005, ****P < 0.0001; two-tailed student's t-test (B); two-tailed Mann–Whitney test (D); two -way ANOVA (A and E). Data are expressed as means \pm SEM.

Figure 6. GABAergic neuronal mitochondria stress requires DAF-16/FoxO to trigger the non-cell-autonomous effects.

(A) Lifespan analysis to evaluate the role of *daf-16* in the extended lifespan induced by *Pgaba::isp-1* dsRNA. The significance of the lifespan curves was assessed using a Log-rank (Mantel-Cox) test. (B and C) Stress tolerance assays. In a *daf-16(mgDf47)* mutant background, *Pgaba::isp-1* dsRNA expression failed to increase resistance to heat stress (B) or paraquat stress (C) compared to control EV gRNAi. (D and E) Representative images (D) and quantification (E) of mitochondrial membrane potential assessed by MitoTracker Red CMXRos dye staining at 3-day-old adults. (F and G) Representative images (F) and quantification (G) of MitoTracker FM Green fluorescent staining at 3-day-old adults to monitor mitochondria mass. (H and I) Relative mtDNA copy number (H) and *polg-1* gene expression level (I) were analyzed by qPCR in EV(gRNAi) and *isp-1(gRNAi)* under *daf-16(mgDf47)* null mutant background. (J) Comparison of the mean number

of eggs laid each day between *daf-16(mgDf47)+isp-1(gRNAi)* and control *daf-16(mgDf47)*; EV*(gRNAi)* animals. (K) The total number of embryos in fertile *daf-16(mgDf47)+isp-1(gRNAi)* and control *daf-16(mgDf47)*; EV*(gRNAi)* animals. Each dot represents an individual animal (E, G, J, and K). Statistical significance is indicated as follows: *P < 0.05, **P < 0.005, ***P < 0.0005, ****P < 0.0001; a one-way ANOVA test for B and C, and a two-tailed Mann–Whitney test for E, G, H, I, J, and K. Data are expressed as means ± SEM. Bars, 50 μm.

Figure 7. Non-cell autonomous effects of GABAergic neuronal mitochondrial stress were

not additively enhanced by the loss of GABA signaling.

(A) Lifespan analysis was conducted on animals with indicated genetic backgrounds to investigate

the relationship between GABA signaling and mitochondrial stress in GABAergic neurons. (B and

C) Paraquat and thermal stress assays were performed on unc-25 null mutants with and without

GABAergic neuronal mitochondrial stress induced by Pgaba::isp-1 dsRNA expression to

elucidate their relationship. (D) Assessment of the fluorescence intensity of the Psod-3::GFP

reporter, indicative of DAF-16/FoxO activity, in the specified mutants. (E) Evaluation of aldicarb

sensitivity in response to the expression of isp-1 dsRNAs in GABAergic neurons. Each dot

represents an individual group in B, D, and E and individual animal in D. *P < 0.05, **P < 0.005,

P < 0.005, *P < 0.001; Log-rank (Mantel-Cox) test for A; one-way ANOVA test for B, C, D,

and E. Data were expressed as means ± SEM.

Figure 8. FLP-13 neuropeptides modulate organismal lifespan and stress tolerance,

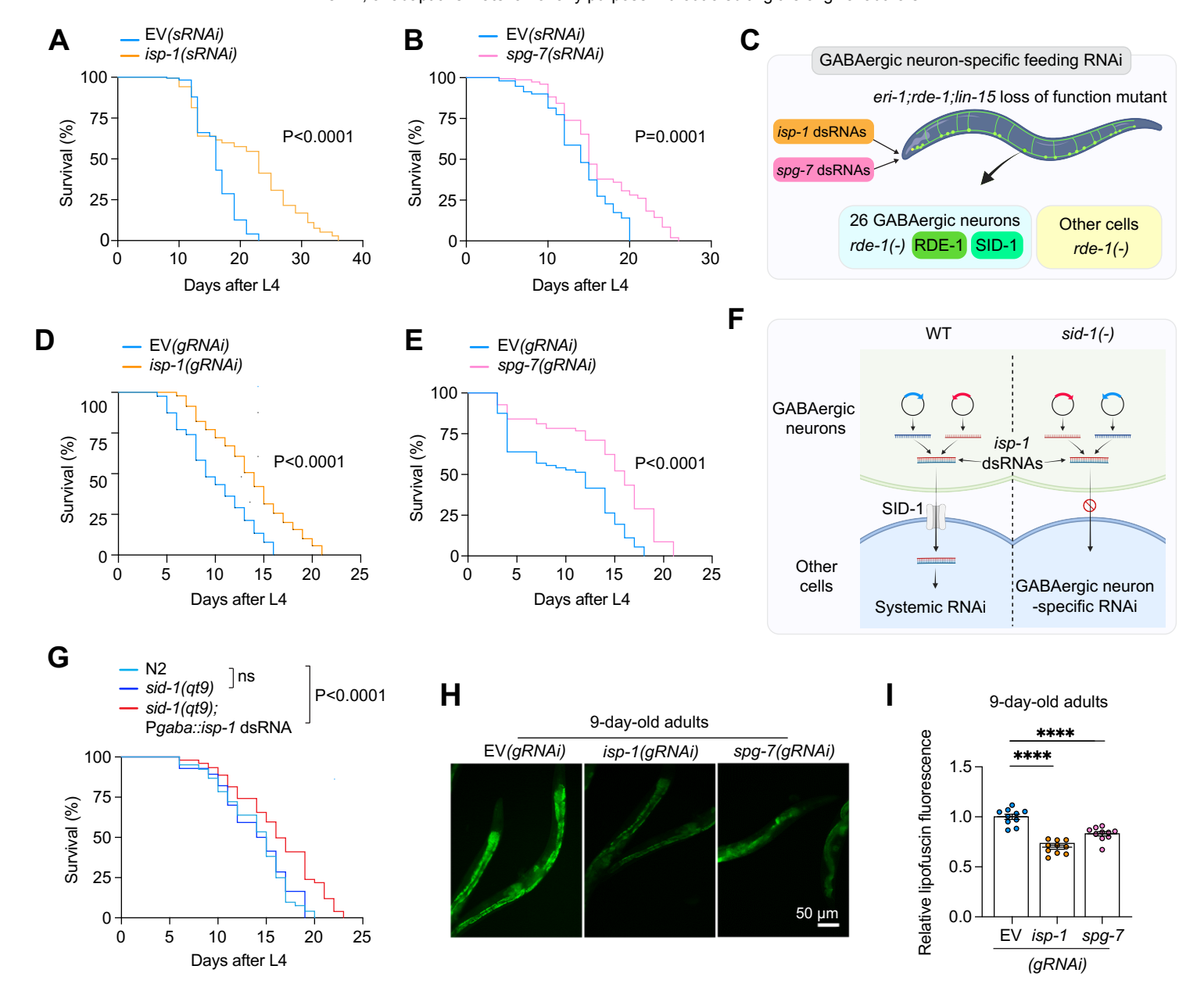
without expanding the non-cell autonomous effects of GABAergic neuronal mitochondrial

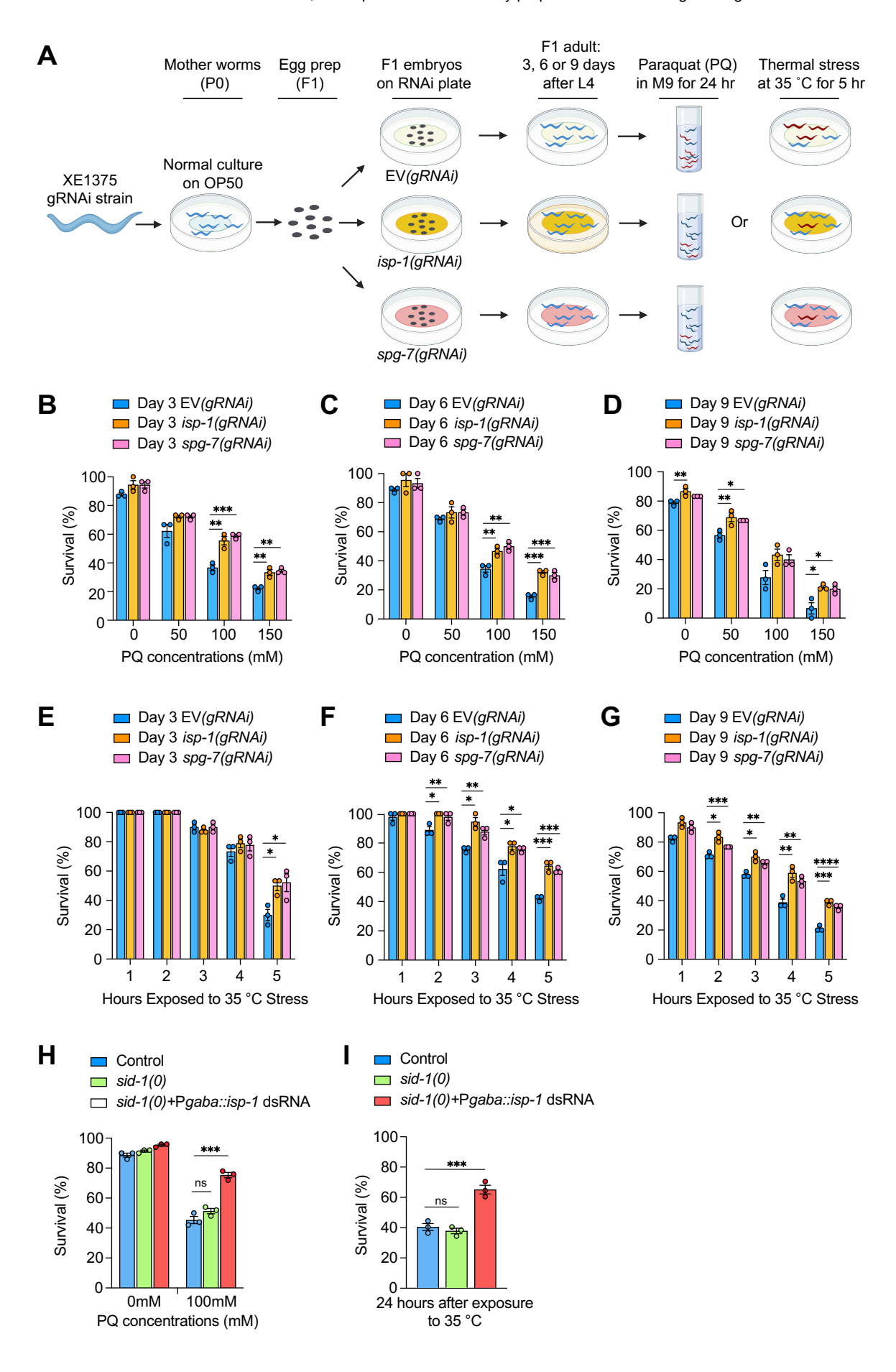
stress. (A and B) Lifespan assays were conducted to evaluate the role of unc-31 (A) and flp-13

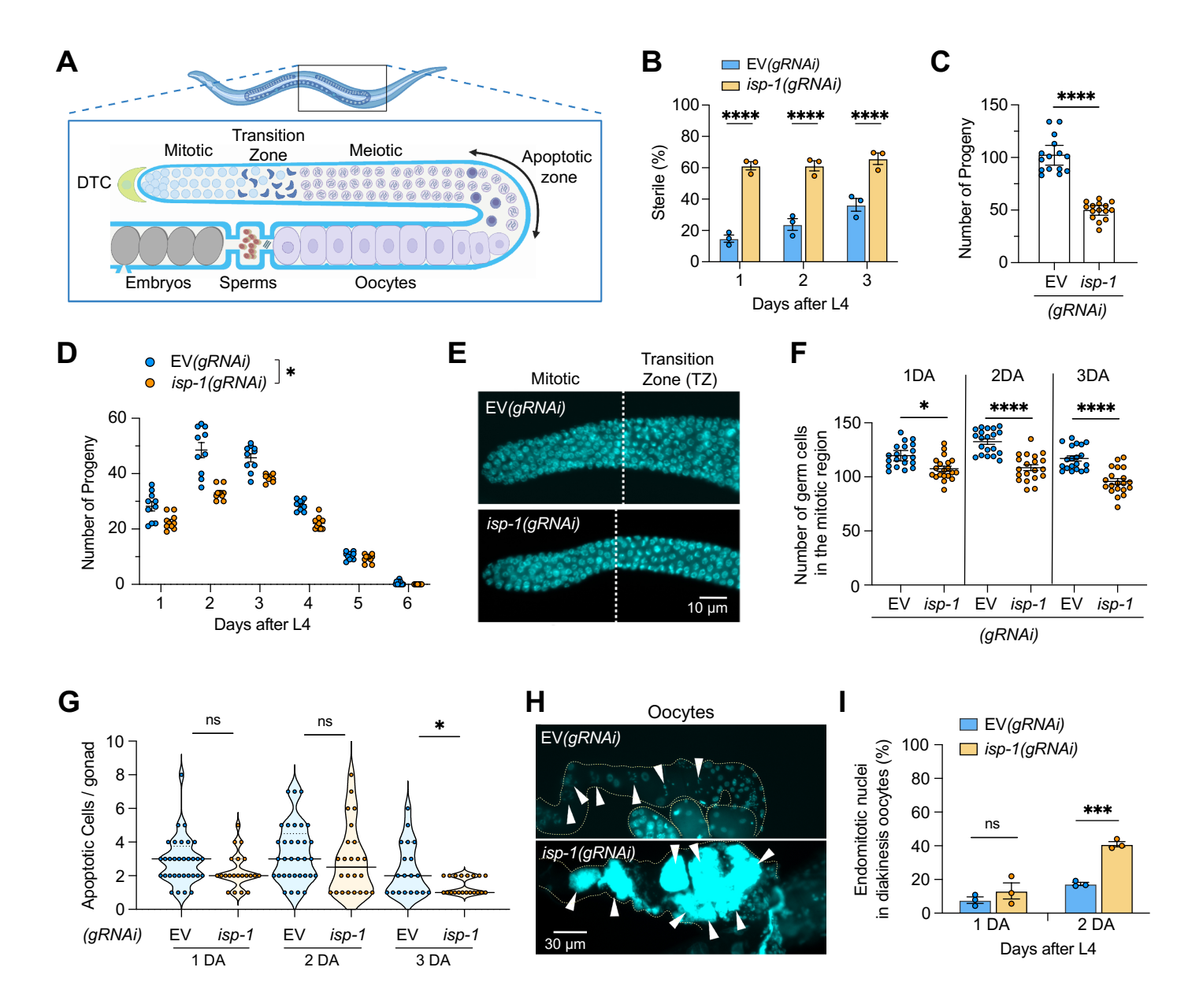
(B) in regulating organismal longevity. (C and D) Quantitative analysis of the thermal (C) and

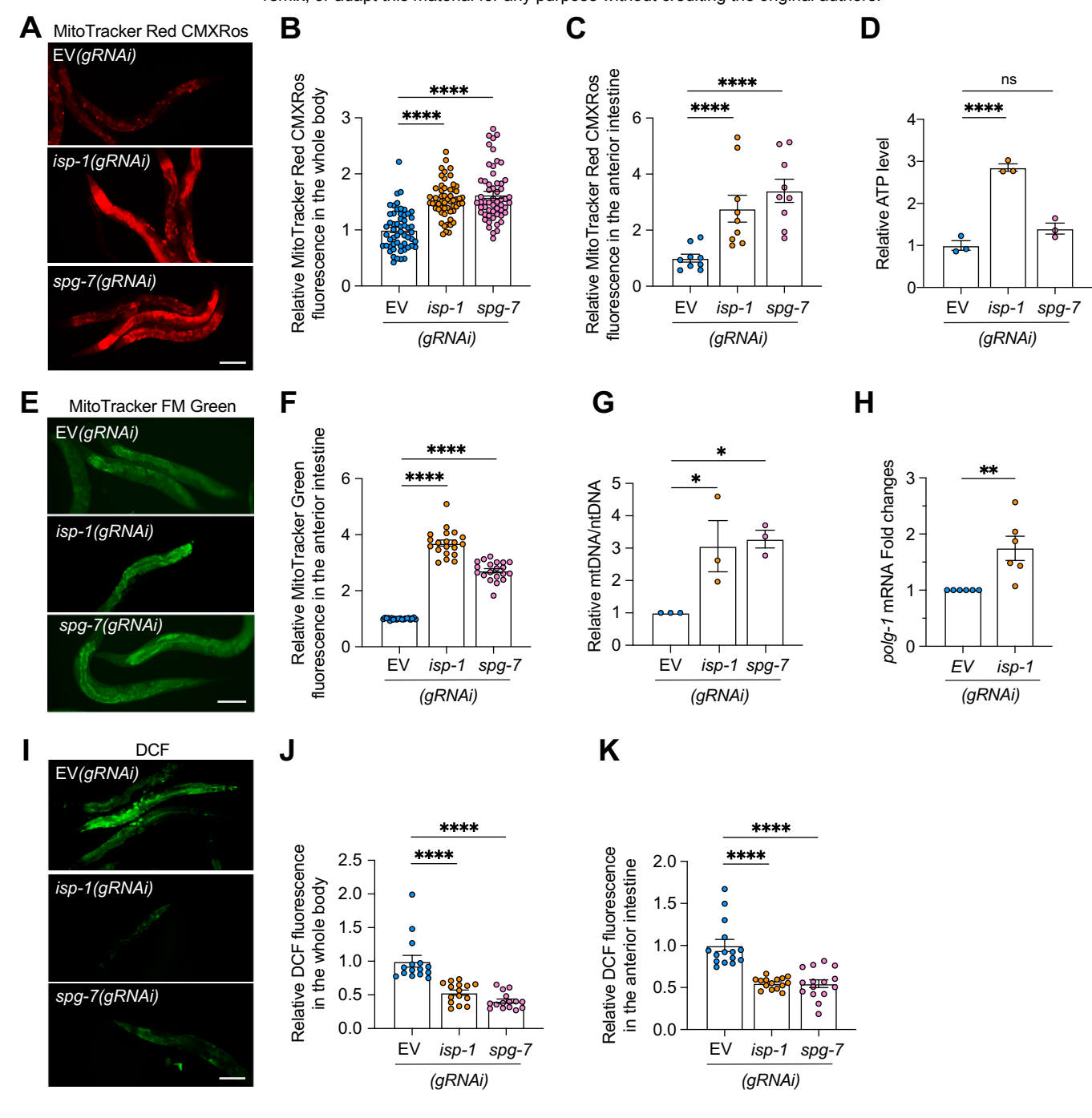
paraquat (D) stress resistance assays was performed after double gRNAi, induced by feeding

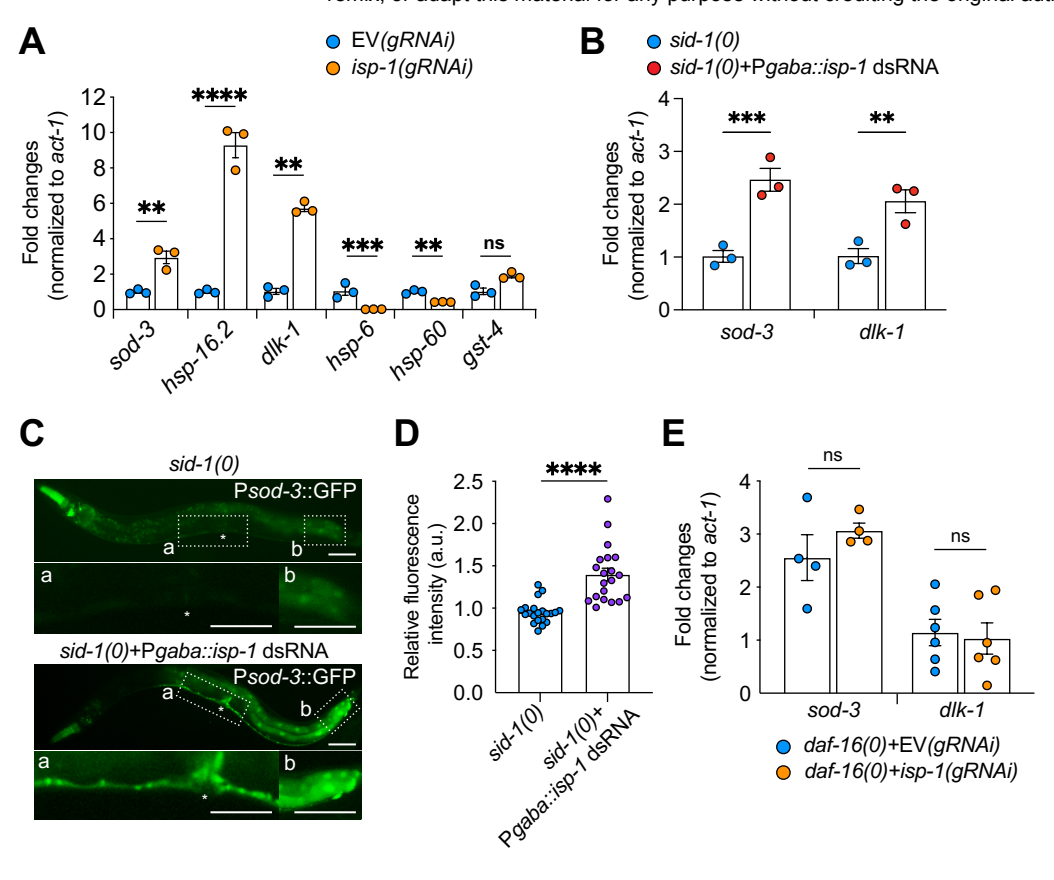
worms a 50:50 mixture of two bacterial strains expressing either EV, *flp-13*, or *isp-1* dsRNAs. *P < 0.05, **P < 0.005, ***P < 0.005, ***P < 0.001; Log-rank (Mantel-Cox) test for A and B; one-way ANOVA test for H and I. Data were expressed as means ± SEM.

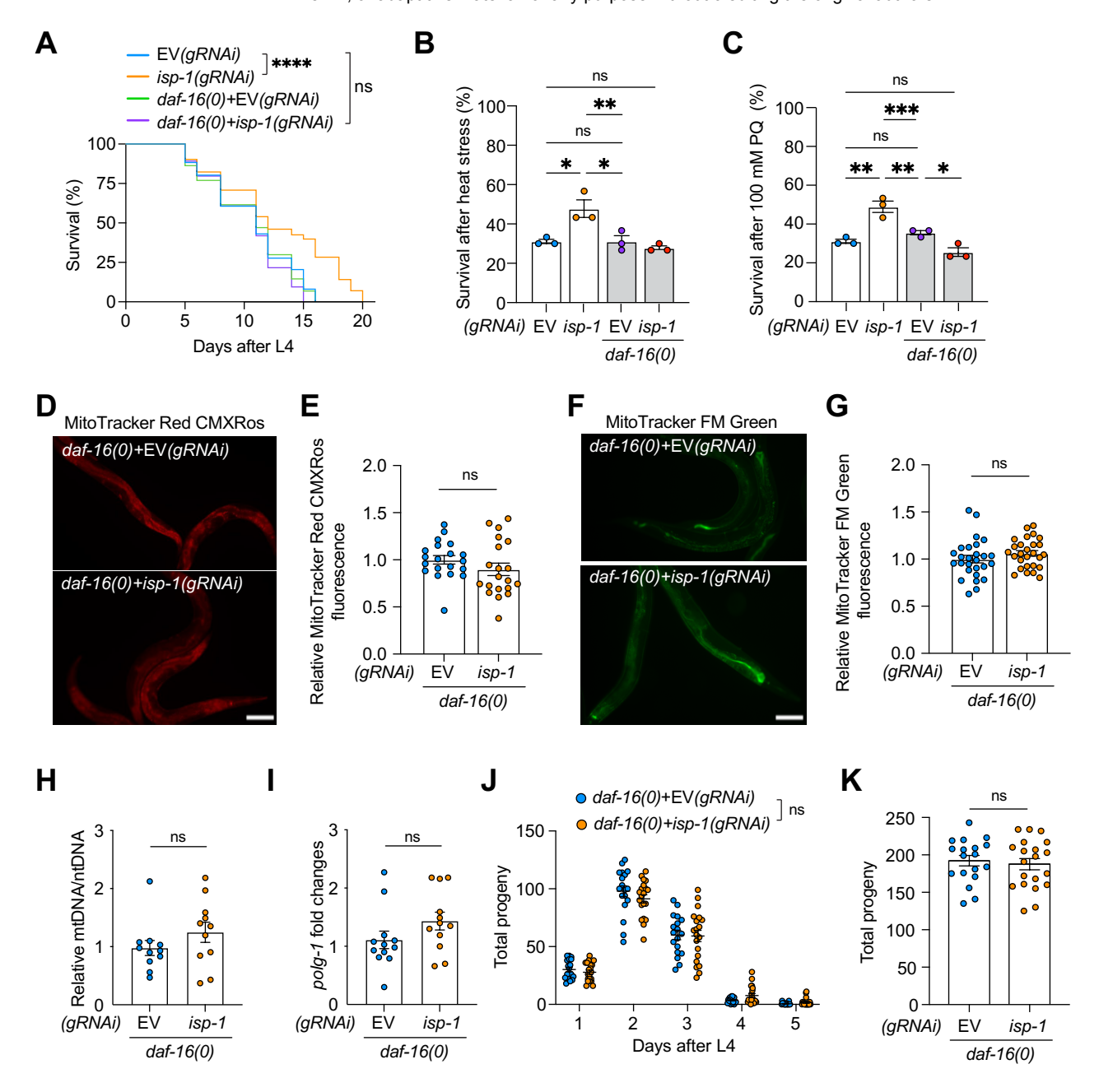


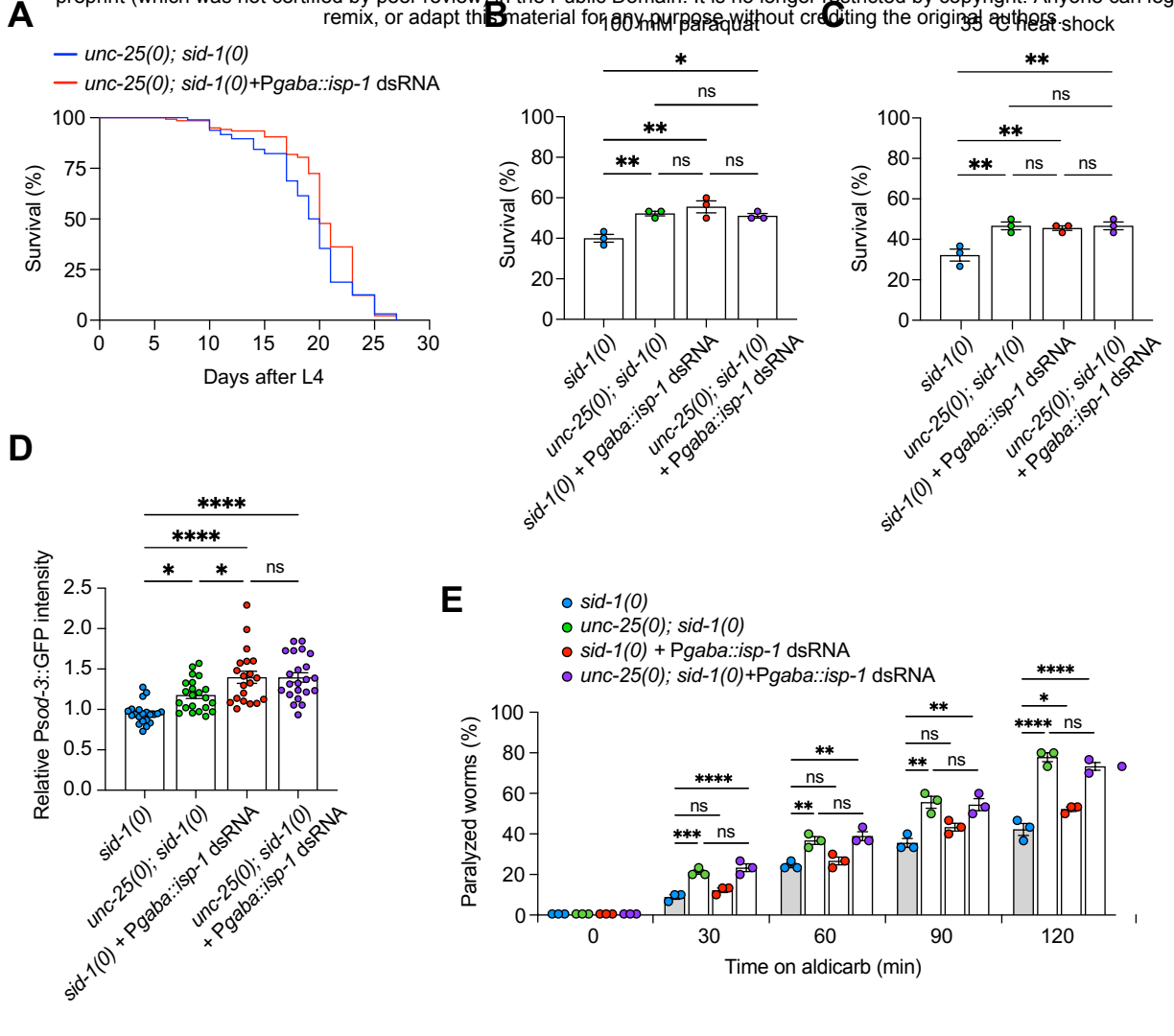


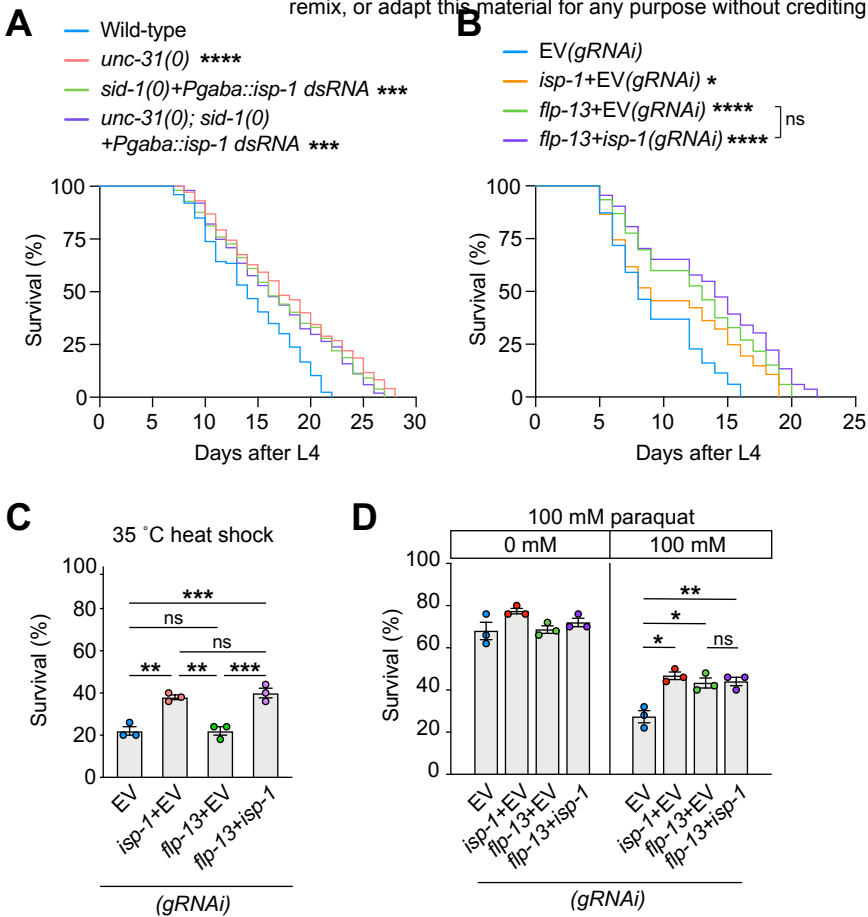












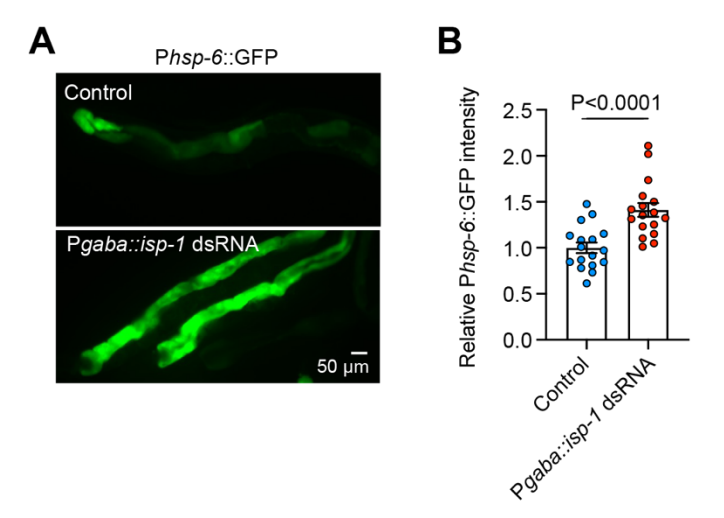


Figure S1. (Related to Figure 1). Global induction of mitoUPR reporter upon *isp-1* dsRNAs expression in GABAergic neurons of wild-type animals.

(A) Representative image showing the increased expression of Phsp-6::gfp transgene in the animals with transcription of isp-1 sense and antisense RNAs in vivo under the GABAergic neuron-specific promoter. Note that the N2 wild-type background allowed the systemic RNAi effects on peripheral tissues. (B) Quantitation of the Phsp-6::GFP fluorescence intensity in the intestine showing the non-cell-autonomous effects of in vivo transcription of isp-1 dsRNAs in GABAergic neurons. Each dot represents an individual animal. Data were expressed as means ± SEM. A two-tailed Mann–Whitney test.

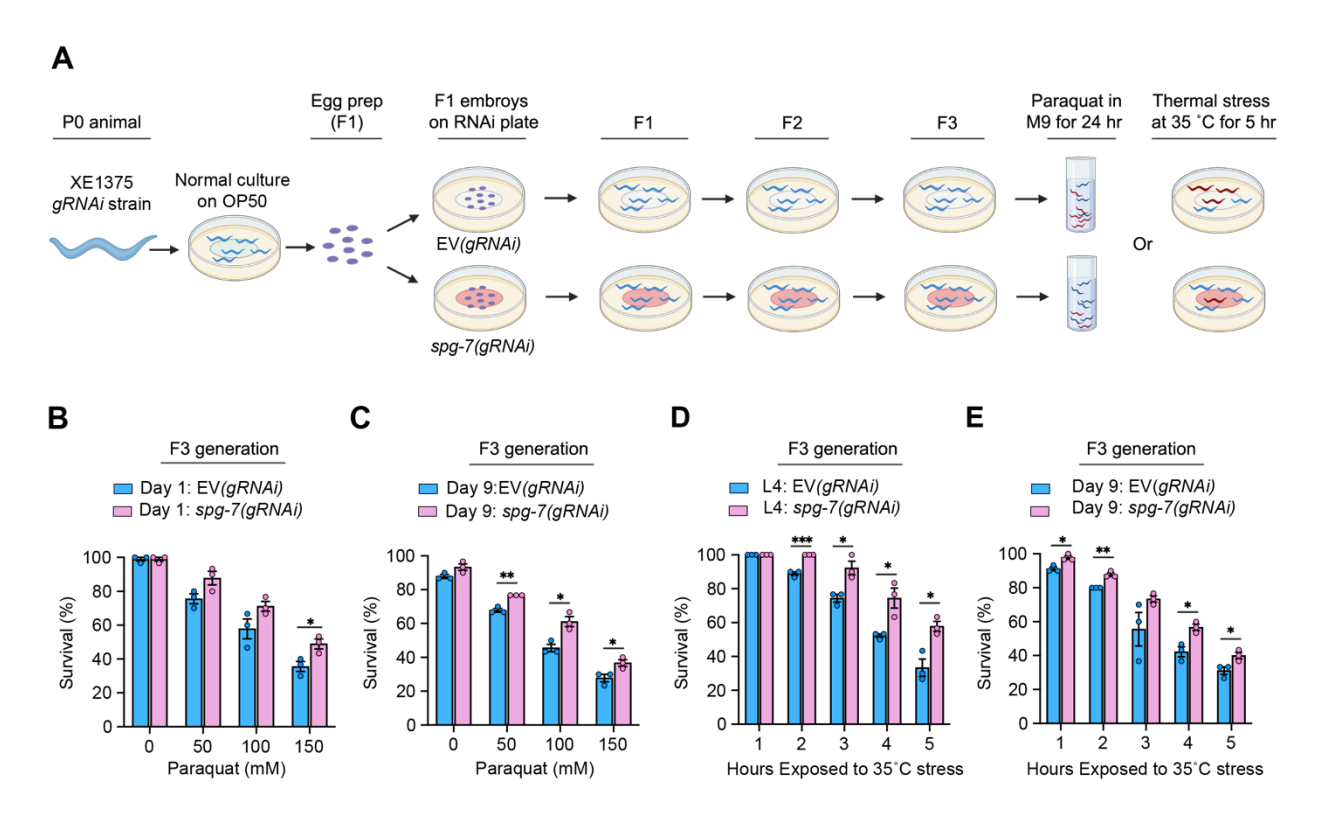


Figure S2. (Related to Figure 2). Continuous gRNAi against *spg-7* over three generations led to altered organismal stress resistance.

(A) A diagram showing the experimental procedure of paraquat and thermal stress response assays in spg-7(gRNAi) animals after continuous RNAi for three generations. (B and C) Quantification of paraquat stress assays in spg-7(gRNAi) animals at 1-day or 9-day-old adult stages. (D and E) Quantification of thermal stress assays in spg-7(gRNAi) animals at the L4 and 9-day-old adult stages. Animals were exposed to 35 °C for 5 hours. Data were expressed as means \pm SEM. *P.<0.05, **P.<0.005, ***P.<0.005, ***P.<0.001; two-tailed student's t-test. Created with https://www.biorender.com/.

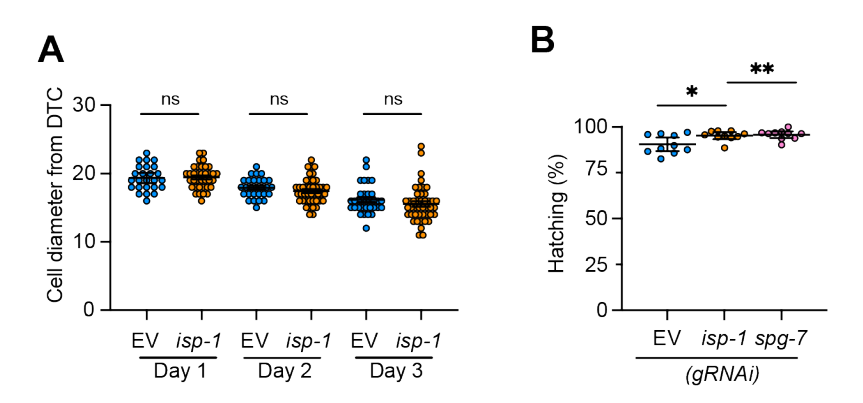


Figure S3. (Related to Figure 3). Non-cell autonomous effects of GABA neuronal mitochondrial stress on the reproductive system.

(A) Diameter of the mitotic area in the distal gonad in *isp-1(gRNAi)* animals. (B) Hatching rates of embryos in *isp-1(GABA-RNAi)* and *spg-7(GABA-RNAi)* animals. *P.<0.05, **P.<0.005; a two-tailed Mann–Whitney test for A; ne-way ANOVA test for B. Data were expressed as means ± SEM.

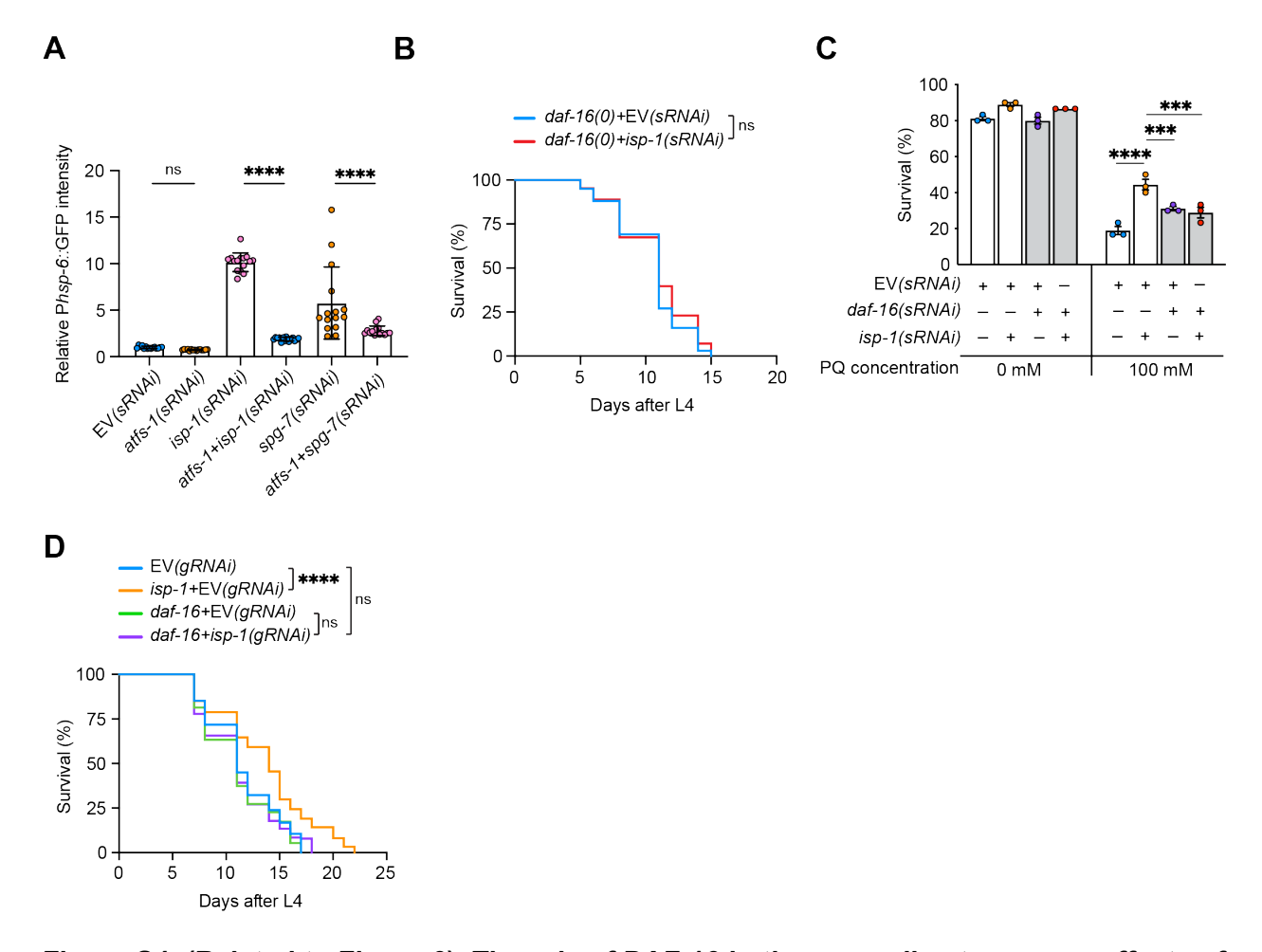


Figure S4. (Related to Figure 6). The role of DAF-16 in the non-cell autonomous effects of GABA neuronal mitochondrial stress.

(A) Quantification of the Phsp-6::GFP intensity in the indicated sRNAi strains. (B and C) Lifespan (B) and paraquat tolerance (C) assays of isp-1 sRNAi under the *daf-16(mgDf47)* null mutant background. (D) Lifespan was tested after gRNAi induction by feeding GABAergic neuronal-specific RNAi strain (XE1375) worms with a 50:50 mixture of bacteria producing either EV, *isp-1*, or *daf-16* dsRNAs.*P.<0.05, **P.<0.005, ***P.<0.005, ***P.<0.001; a two-tailed Mann–Whitney test was used for A; Log-rank (Mantel-Cox) test for B and D; one-way ANOVA test for C. Data were expressed as means ± SEM.

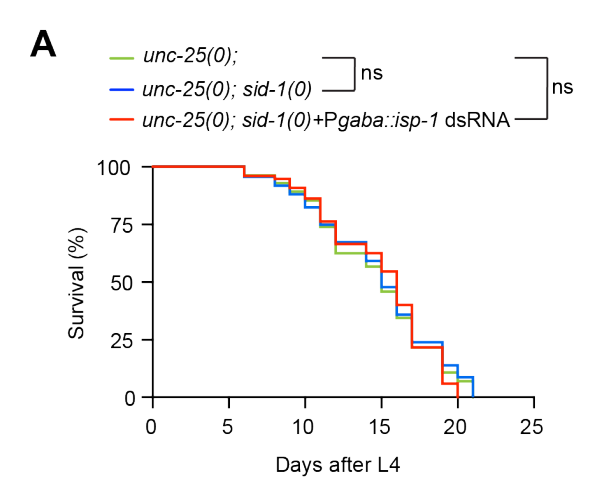


Figure S5 (Related to Figure 7): Assessing the impact of mitochondrial stress in GABAergic neurons on lifespan in *unc-25* null mutants.

(A) Repeated lifespan analysis of *unc-25(qt9)* mutants with and without *isp-1(sRNAi)*. The significance was analyzed by a Log-rank (Mantel-Cox) test.

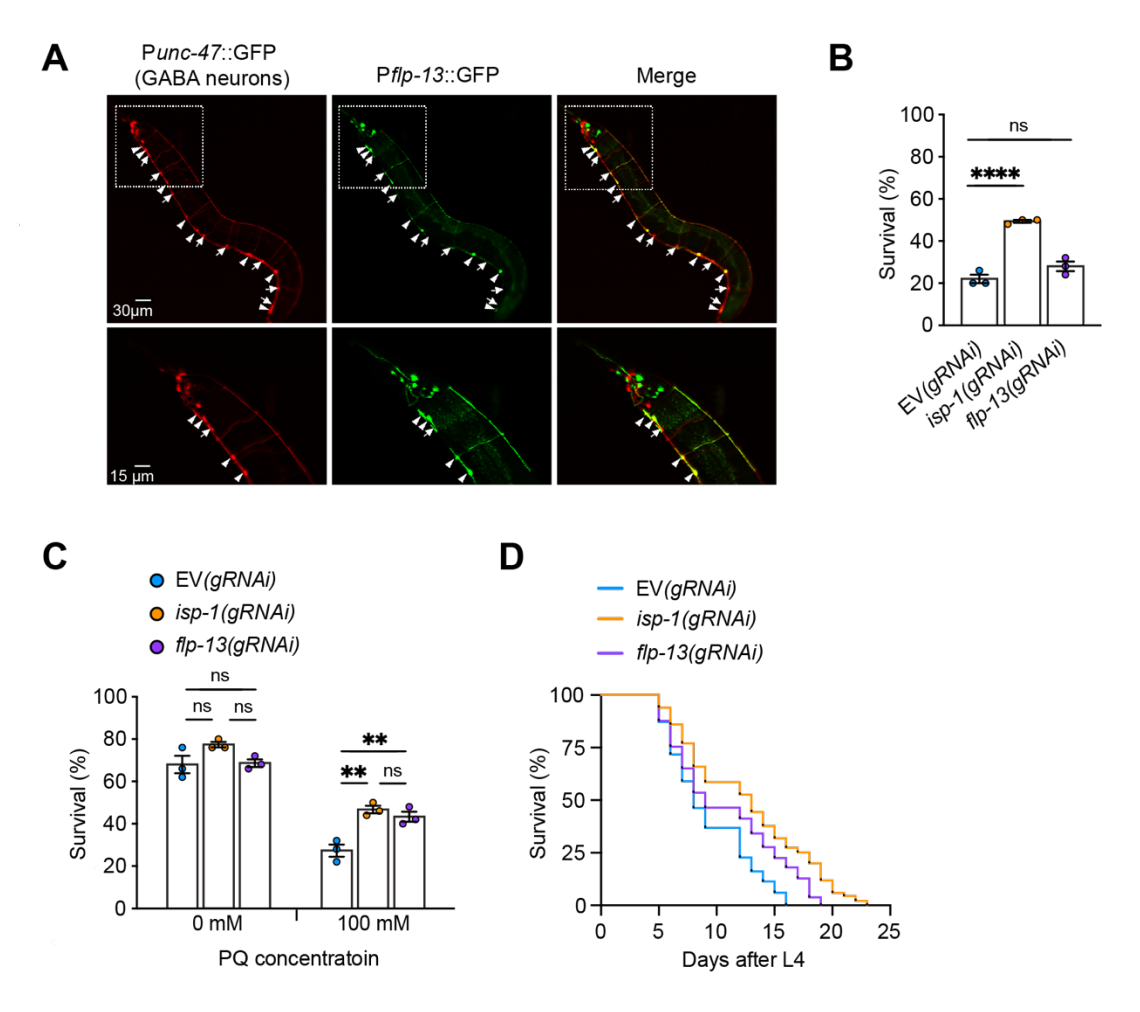


Figure S6. (Related to Figure 8). The effects of single GABA-RNAi inhibition against *flp-13* and *isp-1* on lifespan and stress response.

(A) Representative images of Pflp-13::GFP expression. GABA neurons are visualized by mCherry derived by *unc-47* promoter. Arrowheads indicate the cell body of GABA neurons on the ventral nerve cord with GFP expression. Arrows indicate the cell bodies only with mCherry signals. The dashed boxes are magnified below. (A, B, and C) Lifespan and stress tolerance were tested after gRNAi induction by feeding GABAergic neuronal-specific RNAi strain (XE1375) worms with bacteria producing either *isp-1* or *flp-13* dsRNAs alone for each condition. (B) The survival rate after incubation at 35°C for 5 hours was measured in animals at the 3-day-old adult stage. At least 30 animals were tested for each set. (C) The survival rate of animals cultured in indicated concentrations of paraguat for 24 hours was measured at the 3-day-old adult stage. (D) Lifespan

assay of isp-1(gRNAi) and flp-13(gRNAi) animals. **P < 0.005, ****P < 0.001; one-way ANOVA test for B and C; a Log-rank (Mantel-Cox) test for D. Data were expressed as means \pm SEM.

Table S1. Related to Figs. 1, 6, 7, S4, and S5. Lifespan summary. For P values, stars in the 'Genotype' column are provided to denote the genotype (within the group delimited by color) against which the comparison was performed. Actual P values are provided in the 'significance' column. The results indicate the total lifespan summary of triplicates.

Related Figure	Background genotype	RNAi treatment against	Median lifespan (days)	No. of total worms	P (Log-rank test)
Figure 1A	Wild-type N2	EV	16	174	
		isp-1	23	172	P < 0.0001
Figure 1B	Wild-type N2	EV	14	150	
		spg-7	15	153	P = 0.0001
Figure 1D	wpls36 I; wpSi1 II; eri-1(mg366) IV; rde-1(ne219) V; lin- 15B(n744) X	EV	9	127	
		lsp-1	14	140	<i>P</i> < 0.0001
Figure 1E	wpls36 I; wpSi1 II; eri-1(mg366) IV; rde-1(ne219) V; lin- 15B(n744) X	EV	12	72	
		spg-7	16	69	P < 0.0001
Figure 1G	*Wild-type N2		15	144	
	**sid-1(qt9)		14.5	140	*P = 0.59
	sid-1(qt9)	Pgaba::isp-1 dsRNA	16	151	*P < 0.0001 **P < 0.0001
Figure 6A	wpls36 I; wpSi1 II; eri-1(mg366) IV; rde-1(ne219) V; lin- 15B(n744) X	*EV	11	137	
		**isp-1	12	113	*P < 0.0001
	daf-16(mgdf47) wpls36 I; wpSi1 II; eri-1(mg366) IV; rde-1(ne219) V; lin-15B(n744) X)	***EV	11	117	*P = 0.77
		isp-1	11	148	*P = 0.045 **P < 0.0001 ***P = 0.097
Figure 7A	unc-25(e156); sid-1(qt9)		19.50	96	
	unc-25(e156); sid-1(qt9)	Pgaba::isp-1 dsRNA	20	138	P=0.0029
Figure 8A	*Wild-type N2		14	126	
	**unc-31(e928)		17	145	*P < 0.0001
	***sid-1(qt9)	Pgaba::isp-1 dsRNA	16	154	*P < 0.0001 **P = 0.11
	unc-31(e928); sid-1(qt9)	P <i>gaba::isp-1</i> dsRNA	16	151	*P < 0.0001 **P = 0.04 ***P = 0.59
Figure 8B		*EV	8	149	

	wpls36 l; wpSi1 ll; eri-1(mg366) IV; rde-1(ne219) V; lin- 15B(n744) X	**isp-1+EV	9	149	*P < 0.0001
		***flp-13+EV	13	152	*P < 0.0001 **P = 0.008
		flp-13+isp-1	14	135	*P < 0.0001 ** P < 0.0001 *** P = 0.02
Figure S4B	daf-16(mgdf47)	*EV	11	100	
	daf-16(mgdf47)	isp-1	11	126	* <i>P</i> =0.16
Figure S4D	wpls36 l; wpSi1 II; eri-1(mg366) IV; rde-1(ne219) V; lin- 15B(n744) X	*EV	11	142	
		**isp-1+EV	14	147	*P = 0.0001
		***daf-16+ EV	11	150	
		daf-16 + isp-1	11	140	*P = 0.76 **P < 0.0001 ***P = 0.48
Figure S5A	*unc-25(e156)		15	157	
	**unc-25(e156); sid-1(qt9)		16	152	*P=0.72
	unc-25(e156); sid-1(qt9)	Pgaba::isp-1 dsRNA	15	159	*P=0.56 **P=0.31
Figure S6D	wpls36 I; wpSi1 II; eri-1(mg366) IV; rde-1(ne219) V; lin- 15B(n744) X	*EV	8	149	
		**isp-1	13	135	*P<0.0001
		flp-13	9	155	*P<0.0001 ** P=0.0001